AFCRL--65-307

EXPERIMENTAL AND THEORETICAL STUDY OF TERRESTRIAL AND PLANETARY ATMOSPHERES

Submitted by

K. Watanabe

Hawaii Institute of Geophysics
and
Department of Physics
University of Hawaii
Honolulu, Hawaii

Contract No. AF19(628)-265

Project No. 8627

Task No. 862701

FINAL REPORT

Date of Report - April 15, 1965

Period Covered: 1 February 1962 - 31 March 1965

Prepared

for

AIR FORCE CAMBRIDGE RESEARCH LABORATORIES
OFFICE OF AEROSPACE RESEARCH
UNITED STATES AIR FORCE
BEDFORD, MASSACHUSETTS

Requests for additional copies by agencies of the Department of Defense, their contractors, or other government agencies should be directed to:

DEFENSE DOCUMENTATION CENTER (DDC)
CAMERON STATION
ALEXANDRIA, VIRGINIA 22314

Department of Defense contractors must be established for DDC services or have their "need-to-know" certified by the cognizant military agency of their project or contract.

All other persons and organizations should apply to the:

Clearinghouse for Federal Scientific
and Technical Information (CFSTI)
Sills Building
5285 Port Royal Road
Springfield, Virginia 22151

AFCRL--65-307

EXPERIMENTAL AND THEORETICAL STUDY OF TERRESTRIAL AND PLANETARY ATMOSPHERES

Submitted by

K. Watanabe

Hawaii Institute of Geophysics
and
Department of Physics
University of Hawaii
Honolulu, Hawaii

Contract No. AF19(628)-265

Project No. 8627

Task No. 862701

FINAL REPORT

Date of Report - April 15, 1965

Period Covered: 1 February 1962 - 31 March 1965

Prepared

for

AIR FORCE CAMBRIDGE RESEARCH LABORATORIES
OFFICE OF AEROSPACE RESEARCH
UNITED STATES AIR FORCE
BEDFORD, MASSACHUSETTS

TABLE OF CONTENTS

ABSTRACT		iii
LIST OF CONTRIBUTORS		iv
I.	PUBLICATION LIST	1
II.	ABSORPTION AND PHOTOIONIZATION COEFFICIENTS OF NH_3 IN THE REGION 580-1650 A, by K. Watanabe and S. P. Sood.	3
III.	ABSORPTION AND PHOTOIONIZATION COEFFICIENTS OF CO_2 IN THE REGION 580-1670 A, by R. S. Nakata, K. Watanabe, and G. M. Gnanapragasam.	34
IV.	PHOTOIONIZATION AND ABSORPTION COEFFICIENTS OF NITRIC OXIDE IN THE REGION 580-1100 A, by F. M. Matsunaga, J. S. Sasser, and K. Watanabe.	60
V.	MISCELLANEOUS TOPICS	78
	1. Absorption Coefficient of H_2 in the Region 600-840 A	78
	2. Ionization Potential of COS	82
	3. Fluorescence and Scattering of Some Gases Under Excitation of 1100-2200 A Radiation	84

ABSTRACT

Part I lists the title and abstract of six papers which resulted from this contract.

Part II presents absorption and photoionization coefficients of NH_3 in the region 580-1650 A obtained with improved resolution. Both the Hopfield helium continuum and H_2 emission sources were used. An ionization potential of 10.166 eV is proposed on the basis of Rydberg band analysis.

Part III presents both coefficients of CO_2 over the region 580-1670 A determined by the same methods. Photoionization efficiencies range from 60 to 95 per cent, and most bands below 900 A are preionized. The doublet ionization potential (13.786 and 13.766 eV) is confirmed.

Part IV presents k and k_i values of NO in the region 580-1100 A. Most bands are both preionized and predissociated.

An absorption curve of H_2, ionization potential of COS and scattering of vacuum UV radiation are briefly described in Part V.

LIST OF CONTRIBUTORS

Gnanapragasam, G. M. - as M. S. degree student.

Now Assistant Professor, Thiagarajar College, India.

Jackson, R. S. - as M. S. degree student.

Now member of Stanford Research Institute.

Katayama, Daniel - as M. S. degree student.

Now at Air Force Cambridge Research Laboratories.

Matsunaga, F. M. - Junior Physicist.

Metzger, P. H. - Junior Physicist.

Now at Aerospace Corporation, Los Angeles.

Nakata, R. S. - as M. S. degree student.

Sasser, J. S. - as M. S. degree student.

Now at Hawaii Institute of Geophysics,
University of Hawaii.

Sood, S. P. - Assistant Professor of Chemistry.

Watanabe, K. - Professor of Physics and Principal Investigator.

Yokotake, George - Junior Specialist in Physics.

I

PUBLICATION LIST

The following papers resulted from partial or total sponsorship of Contract AF 19(628)-265.

1. "Ionization Potentials of Some Molecules," J. Quant. Spectry. and Rad. Transfer 2, 369 (1962) by K. Watanabe, T. Nakayama, and J. Mottl.

Abstract

This report summarizes the measurements of molecular ionization potential by a photoionization method utilizing a 1 m vacuum monochromator in the photon energy range from 7-15 eV. The adiabatic ionization potentials of about three hundred molecules determined by the present method are assembled in thirteen tables, which include estimates of experimental uncertainties. In nearly all cases (about forty) where comparisons can be made, the present results agree closely with the spectroscopic values. The identity of the most loosely bound electrons, the effect of alkyl substitution, and the relationship between ionization continua and absorption bands are suggested for some of the molecules.

2. "Photoionization Rates in the E and F Regions," J. Geophys. Res. 67, 999 (1962) by K. Watanabe and H. E. Hinteregger.

Abstract

Photoionization rates in the altitude region 90-400 km computed on the basis of recent data on solar ultraviolet intensities are as much as two orders of magnitude larger than previous values. The results contradict the current theory that E-region ionization is due predominently to soft X rays; observed radiation in the spectral range 800-1027 A that ionizes O_2 contributes a greater or comparable photoionization rate. The base of the E region is probably controlled by Lyman β and the C III line at 977 A. The electron production in the F region is primarily due to ultraviolet radiation in the range 170-900 A. At sunrise the maximum ionization rate is at about 320 km but descends to about 150 km for zenith sun. The F_1 ledge probably follows this maximum and descends to about 150 km. The F_2 peak is apparently due to the combined result of the daytime enhancement of electron density and the slow recombination.

3. "Photoionization Rates in the E and F Regions, 2" J. Geophys. Res. 67, 3373 (1962) by H. E. Hinteregger and K. Watanabe.

Abstract

The study of photoionization rates in the E and F regions is re-examined in the light of vertical and spectral distribution of the observed photon absorption rate densities of Aug. 23, 1961. The results of the present study suggest a reasonably unified physical picture of daytime conditions.

4. "Absorption and Photoionization Coefficients of Acetylene, Propyne, and 1-Butyne," J. Chem. Phys. 40, 558 (1964) by T. Nakayama and K. Watanabe.

Abstract

Absorption coefficients of acetylene, propyne and 1-butyne were measured by a photoelectric technique in the region 1050-2000 A. Two or three Rydberg series accompanied by vibrational bands were observed in the spectrum of these molecules. The photoionization curves and the Rydberg series yielded the same ionization potential: 11.41, 10.36, and 10.18 eV for acetylene, propyne and 1-butyne, respectively.

5. "Absorption and Photoionization Cross Section of H_2O and H_2S," J. Chem. Phys. 41, 1650 (1964) by K. Watanabe and A. S. Jursa.

Abstract

Absorption and photoionization cross sections of H_2O in the region 850-1110 A and H_2S in the region 1060-2100 A were measured by photoelectric methods. The absorption curves support the photographic study of H_2O and H_2S by Price. The photoionization curves yielded the following ionization potentials: 12.62 eV for H_2O and 10.46 eV for H_2S.

6. "Photoionization Yield and Absorption Coefficient of Xenon in the Region 860-1022 A," J. Quant. Spectry. and Rad. Transfer, in press (1965) by F. M. Matsunaga, R. S. Jackson, and K. Watanabe.

Abstract

Absorption coefficient and absolute photoionization yield of xenon gas have been measured by photoelectric methods with 0.2 A bandwidth in the 860-1022 A region. Ionization yields were obtained with a platinum detector calibrated against a calibrated thermocouple. A yield value of unity was obtained throughout this region which includes preionized Rydberg lines. The absorption coefficient at most wavelengths fell between the spread of previous values.

II

ABSORPTION AND PHOTOIONIZATION COEFFICIENTS OF NH_3 IN THE REGION 580-1650 A

By K. Watanabe and S. P. Sood

1. INTRODUCTION

Early studies of the absorption spectrum of ammonia in the vacuum ultraviolet region were made by Leifson[1] (1400-2400 A), Dixon[2] (1900-2400 A), and Duncan[3,4] (800-2300 A). A photograph by Duncan[4] shows a fairly clear picture of the NH_3 absorption spectrum in the region 1200-2200 A. In his detailed study, Duncan[3] classified four extensive band progressions: Series I (1680-2170 A), II (1390-1670 A), III (1220-1440 A), and IV (1160-1210 A). Series I is very diffuse while the others are much sharper and show rotational structure. Duncan and Harrison[5] used a 21-ft spectrograph to investigate the fine structure of seven bands in Series II. Furthermore, Duncan[4] fitted the strongest members of Series I, III, and IV into a Rydberg series and obtained the ionization potential of 11.58 eV (93,380 cm^{-1}). However, this value has not been supported by recent photoionization measurements.[6,7]

Walsh and Warsop[8] reinvestigated the band systems in the region 1100-2200 A and reported a different interpretation of bands in the region below 1330 A. Using the first members of Series III and a new series beginning at 1330 A, they obtained a Rydberg series converging to 10.18 eV (82,150 cm^{-1}) which is in good agreement with the photoionization value,[7] 10.154 eV. Furthermore, they concluded that the upper states of all five

observed electronic transitions are planar. Douglas and Hollas[9] used a 10-m spectrograph to reinvestigate the rotational structure of Series II and also concluded that the upper state of this transition is planar. Their analysis showed that the 1663 A band is the 1-0 band and not the 0-0 band as interpreted previously. Thus, their work clearly showed that further detailed study of other bands must be carried out before we can establish the ionization potential of NH_3.

The absorption coefficients of NH_3 gas have been determined by several investigators: Thompson and Duncan[10] (1250-2200 A), Tannenbaum et al[11] (1700-2200 A), Watanabe et al[6,12] (1050-2200 A), Sun and Weissler[13] (400-1300 A), and Metzger and Cook[14] (600-1000 A). Photoionization cross sections have been measured by Watanabe[6] (1070-1230 A), Walker and Weissler[15] (700-1200 A), and Metzger and Cook[14] (600-1000 A).

Although the results reported by these investigators provide an extensive coverage of the NH_3 absorption intensity, further work is desirable. The NH_3 spectrum in the region 1100-1650 A is rather complex, but all absorption coefficients have been obtained with low resolution. The work of Metzger and Cook[14] shows that the NH_3 spectrum is continuous in the region below 1000 A, so that high resolution is not necessary. However, their results are not in good agreement with other results.[13,15] For example, Walker and Weissler[15] reported ionization efficiency of 100 % at about 700 A, while Metzger and Cook obtained about 70 %.

Using somewhat improved resolution, we have attempted to determine more quantitative absorption coefficients, especially in the region 1100-1650 A, and to provide a more detailed absorption curve which may be helpful to establish the ionization potential. We also report the absorption coefficient and photoionization yield in the region 600-1000 A obtained with a helium continuum source.

2. EXPERIMENTAL

Two 1-meter, normal incidence monochromators, each with a 1200 lines/mm grating, were used in the present study. Monochromator A (radius mount type, built by McPherson Instrument and described previously[16]) provided a resolution of 0.2 A with 20-μ slits and was used for the region 850-1700 A. Monochromator B (Johnson-Onaka type, fabricated in our shop) had a three-stage differential pumping system at the entrance slit and was used for the region 580-1000 A with a helium light source. A resolution of about 0.3 A was obtained with slit widths of 30 and 20 μ, respectively, for the entrance and exit slits. The grating mount was coupled to a flexible cable to permit focusing under operating conditions.

A windowless hydrogen discharge tube[18] was used with Monochromator A. It was operated at 0.35 or 0.4 amp dc with about 800 V across the tube. For the region 580-1000 A, the Hopfield continuum[19] due to emission from molecular helium was used as light source for Monochromator B. Recently, several investigators[20-23] have used this source in conjunction with photoelectric detection.

The helium light source and the entrance slit section are schematically shown in Fig. 1. It is similar to the arrangement used by Metzger and Cook.[24] The main modification is that the capacitor C (0.0018 μF) and the spark gap G including a small mercury lamp (not shown) were built within the light source assembly and shielded. The resistor R (90 k Ω) was mounted inside a 20 kV Manson dc power supply (Model 605) and connected to the light source by a cable. The tungsten electrodes of the spark gap were attached to lucite rods in such a manner that the gap distance can be adjusted during operation of the light source. The repetition rate of gap breakdown was about 6 kc. Commercial (medical) grade helium was flowed through a copper foil trap and a liquid nitrogen trap to the light source and pumped out through the optical slit (S in Fig. 1) via the 3-stage pumping system. For most measurements the pressure was about 120 mm Hg in the light source and 10^{-5} mm Hg in the main chamber of the monochromator. The photon flux through the exit slit was determined by a xenon ion chamber, using our recent result[25] that photoionization yield of xenon is unity, and found to be about 2×10^{7} photons/sec through the exit slit at the peak (810 A) of the Hopfield continuum. This intensity is comparable to that reported by Huffman et al.[22] However, we have used narrower slits so that the present resolution is somewhat better than the 0.5 A used by them and by Cook and Metzger.[23]

Absorption coefficients were measured by a method described previously.[25-27] The absorption chamber was located

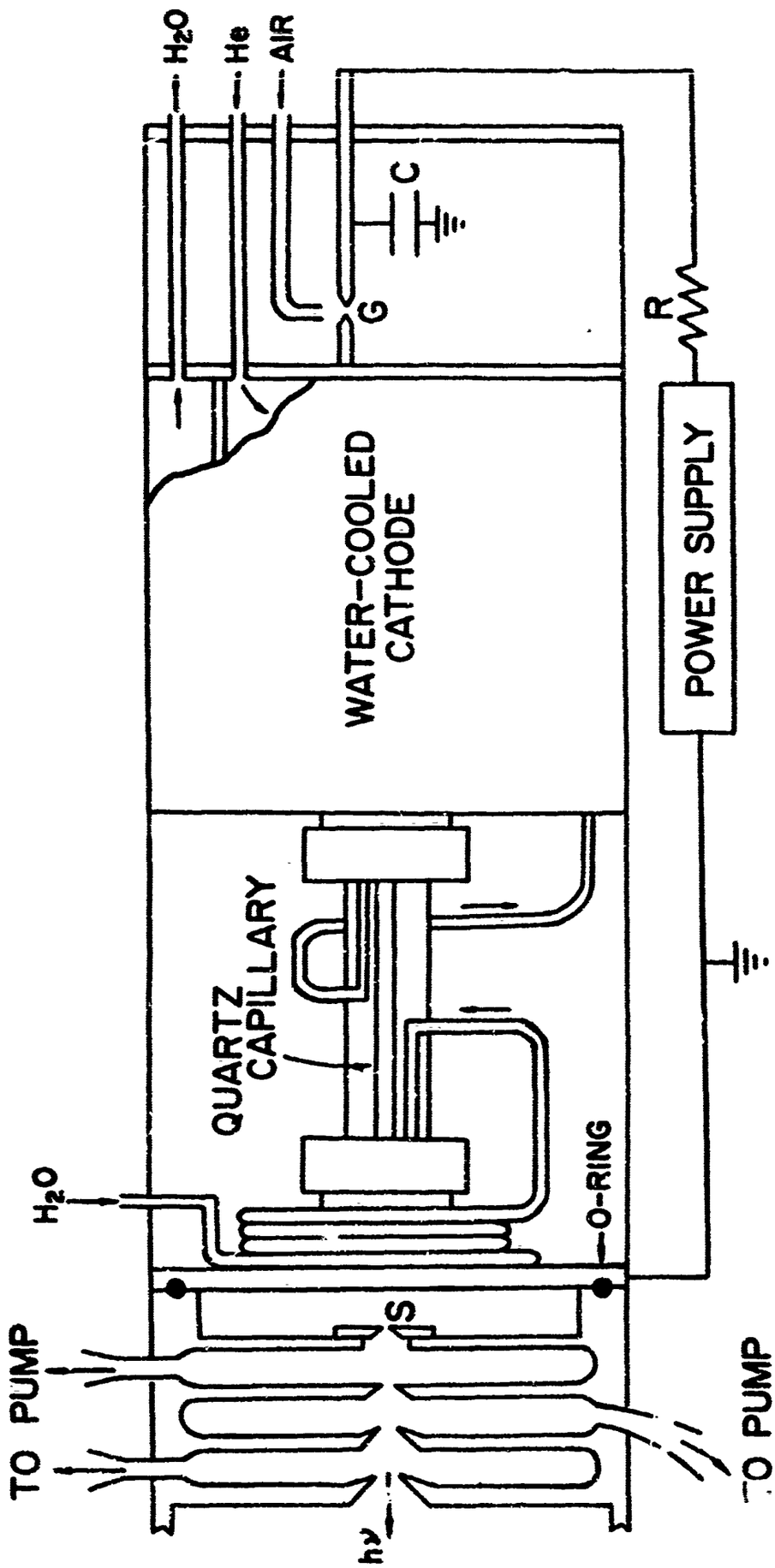

Figure 1. Schematic diagram of light source and differential pumping slits

between the exit slit and a glass plate coated with sodium salicylate, and an EMI 9514B photomultiplier tube was placed in air a few mm behind the glass plate. An absorption cell of length 10.5 cm with LiF windows and parallel plate electrodes was used for the region above 1070 A. For shorter wavelengths the exit slit served as the window and absorption path lengths of 11.5, 13.6, 27.1, and 54 cm were used.

Photoionization yields were determined by comparing the ion current due to a given gas with that of a reference gas with known yield. For the region above 1070 A, the cell with LiF windows was used with nitric oxide as a reference gas.[6,28] To insure total absorption in the ion chamber, relatively high gas pressures were used. For the region below 1020 A, an ion chamber of length 54 cm was used with xenon as a reference gas.[25,29] For most measurements the gas pressures were high enough to give total absorption; however, a photomultiplier placed at the end of the ion chamber continuously measured any transmitted light so that corrections can be applied. A similar method was used by Metzger and Cook.[14,23]

Our study of recently published absorption coefficient of gases in the region below 1000 A suggests that much of the discrepancies may be attributed to systematic error in pressure determination of flowing gas. In order to have a negligible pressure gradient in a flow type absorption chamber, a small exit slit (0.02 x 10 mm^2) and a large chamber dimensions (15 cm diameter and 54 cm length) were used. Moreover, the chamber was opened to a side chamber of 6 liter volume. A Consolidated micromanometer was connected directly to the

absorption chamber. The pressure calibration curve for the manometer obtained with this arrangement was the same as those obtained with shorter cell lengths. In each case the calibration curve was obtained by the following two methods: (a) McLeod gauge using static gas (O_2, N_2 or air) and (b) absorption method[27] using oxygen flowing through the absorption chamber. In the latter method, the absorption coefficient[27] of O_2 was taken as 394 cm^{-1} at 1436.2 A which is in close agreement with recent measurements.[24,30] Calibration curves were obtained from time to time in order to detect any change in the sensitivity of the micromanometer. A typical calibration curve is shown in Fig. 2. The error in our pressure determination is estimated to be less than 5 %.

The NH_3 gas from Matheson Company had a stated purity of 99.99 %. In order to eliminate possible contamination, the sample was redistilled in vacuum four times and transferred to liter flasks. Pressures of gas used were as follows: 0.04 to 15 mm Hg (in the 10.5 cm cell) for the region 1070-1650 A, 0.01 to 0.15 mm Hg (in the 13.7 and 27.1 cm cells) for the region 850-1100 A, 0.05 to 0.20 mm Hg (in the 11.5 and 54 cm cells) for the region 580-1000 A.

The intensity of absorption in this work is expressed by the absorption coefficient k in cm^{-1}. It is defined by the equation $I = I_o \exp(-kx)$ where I_o and I are the incident and transmitted light intensities and x in cm is the layer thickness of absorbing gas converted to 0°C and 1 atm pressure. The photoionization coefficient is defined by $k_i = kY$ where Y is the fractional yield of photoionization.

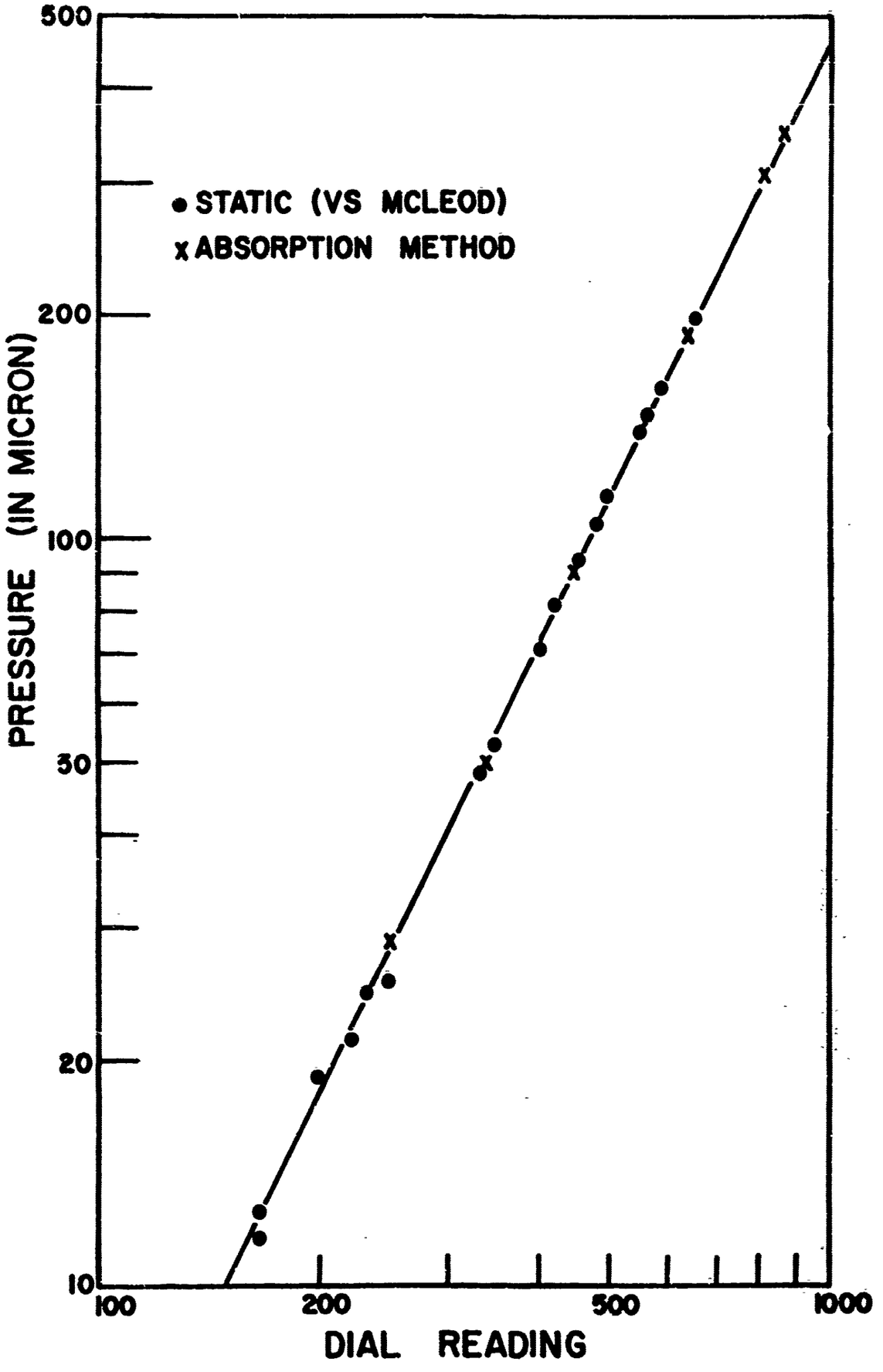

Figure 2. Calibration curve for Consolidated micromanometer

Corrections for scattered light was negligible at many wavelengths but was applied to nearly all wavelengths. With the arrangement used, fluorescence[14] of NH_3 was too weak to be detected and corrections such as used by Huffman *et al*[31] for N_2 was not necessary.

3. RESULTS AND DISCUSSION

a. 580-1000 A Region

The absorption spectrum of NH_3 in this region, as shown in Fig. 3, is merely a broad continuum with a maximum k-value of about 920 cm^{-1} from 700 to 750 A. There is a minimum at about 940 A where the k-value is 420 cm^{-1}. The present k-values for the 580-800 A region fall within the spread of values reported by Sun and Weissler[13] but are as much as 20 °/o higher than those of Metzger and Cook.[14] On the other hand, the present results for the 820-950 A region agree with the latter and are lower than the former. These discrepancies are higher than the estimated error of 10 °/o in our results. The mean k-values listed in Table I show that the spread of values is much less than that of Sun and Weissler who used a line source and photographic photometry. Our recorder traces of the helium continuum showed no fine structure in the NH_3 spectrum in this region.

The photoionization efficiency of NH_3 in the 580-1100 A region is shown in Fig. 4. This result is in good agreement with the data obtained by Walker and Weissler.[15] In fact, their result shows a minimum of about 40 °/o at 850 A and a minor maximum of about 50 °/o at 950 A. This structure

appears clearly in Fig. 4. The curve obtained by Metzger and Cook[14] shows a minimum of about 30 °/o at 850 A; however, in the 580-700 A region where the present yield is about 100 °/o, their values lie between 60 and 70 °/o. Furthermore, their curve does not show the minor peak at 950 A, although they employed the helium source and techniques similar to those used in the present study.

A curve for photoionization coefficient, k_1, is also included in Fig. 3. This curve departs considerably from the curve obtained by Metzger and Cook, the discrepancy being as much as a factor of two at 600 A. Comparison of the k- and k_1-curve in Fig. 3 shows that photoionization and, probably, production of ion pairs ($NH^+ + H_2 + e^-$ and $NH_2^+ + H + e^-$) account for the 100 °/o efficiency in the region below 700 A. The difference betweeen the k- and k_1-curve in the region 700-950 A shows the presence of a dissociation continuum with a maximum at about 830 A.

b. 1000-1180 A Region

The upper curve of Fig. 5 shows the absorption spectrum of NH_3 in this region. The bands in the interval 1150-1180 A are members of band progressions studied by Duncan,[3] and will be discussed in the next section. On the shorter wavelength side, the bands are either very weak or diffuse. Some of these bands, especially in the region 1080-1150 A, are probably members of the long wavelength band progressions. However, we have not attempted to classify them.

The ionization efficiency is 40 °/o at 1000 A, decreases to 33 °/o at 1060 A, rises to 39 °/o at 1095 A, and steadily

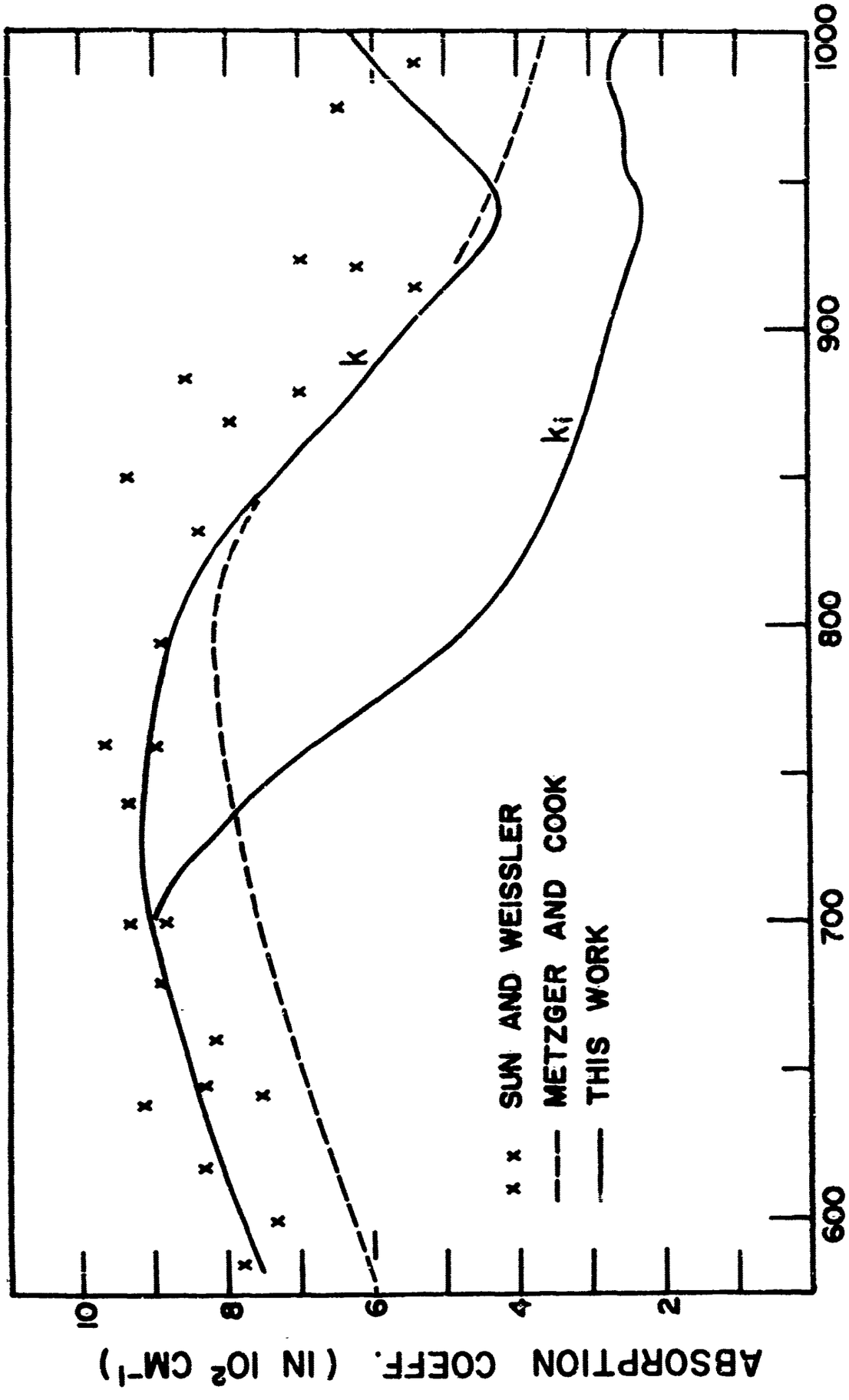

Figure 3. Absorption and photoionization coefficients of NH_3 in the 500 - 1000 A region

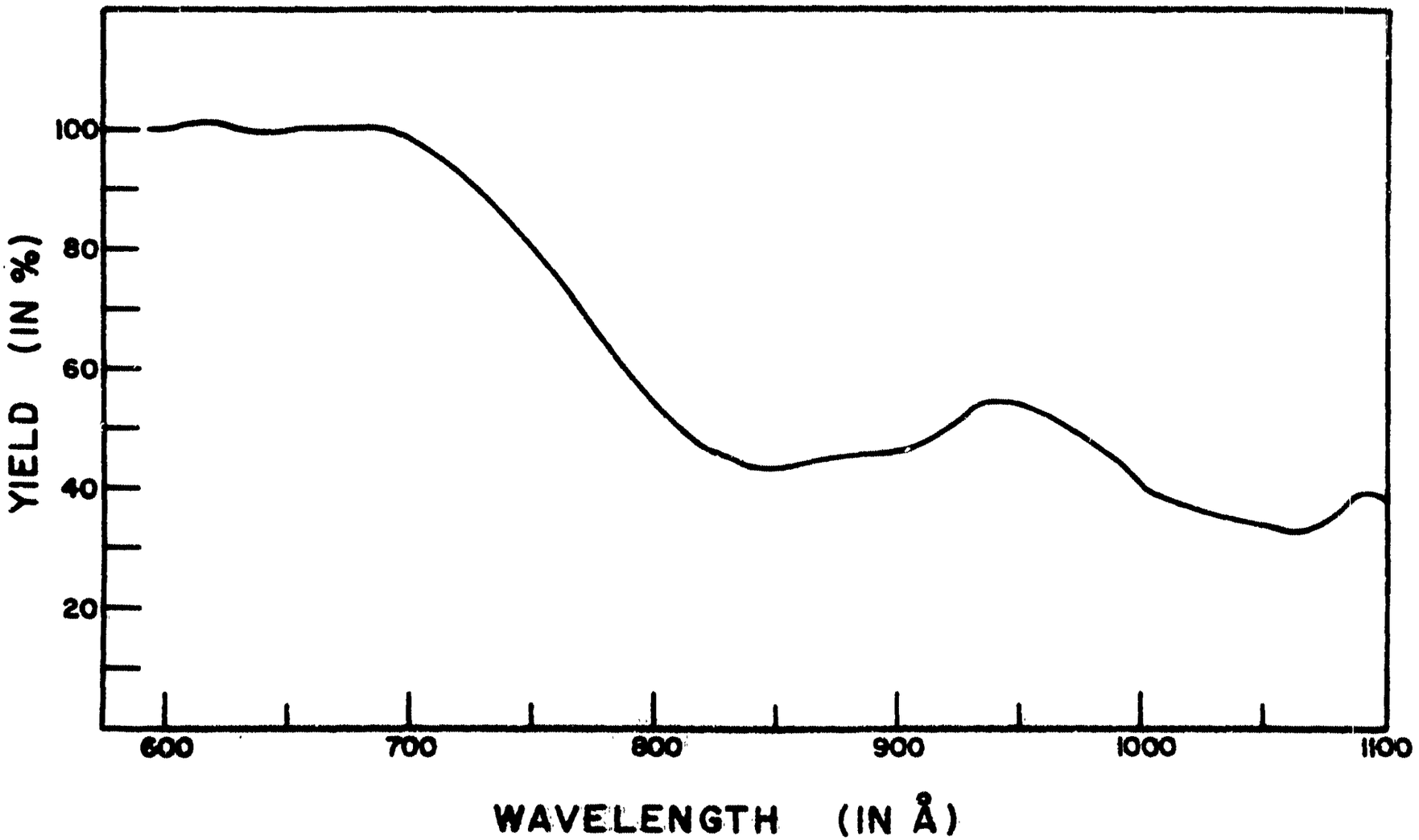

Figure 4. Photoionization efficiency of NH_3 in the region 580 - 1100 A

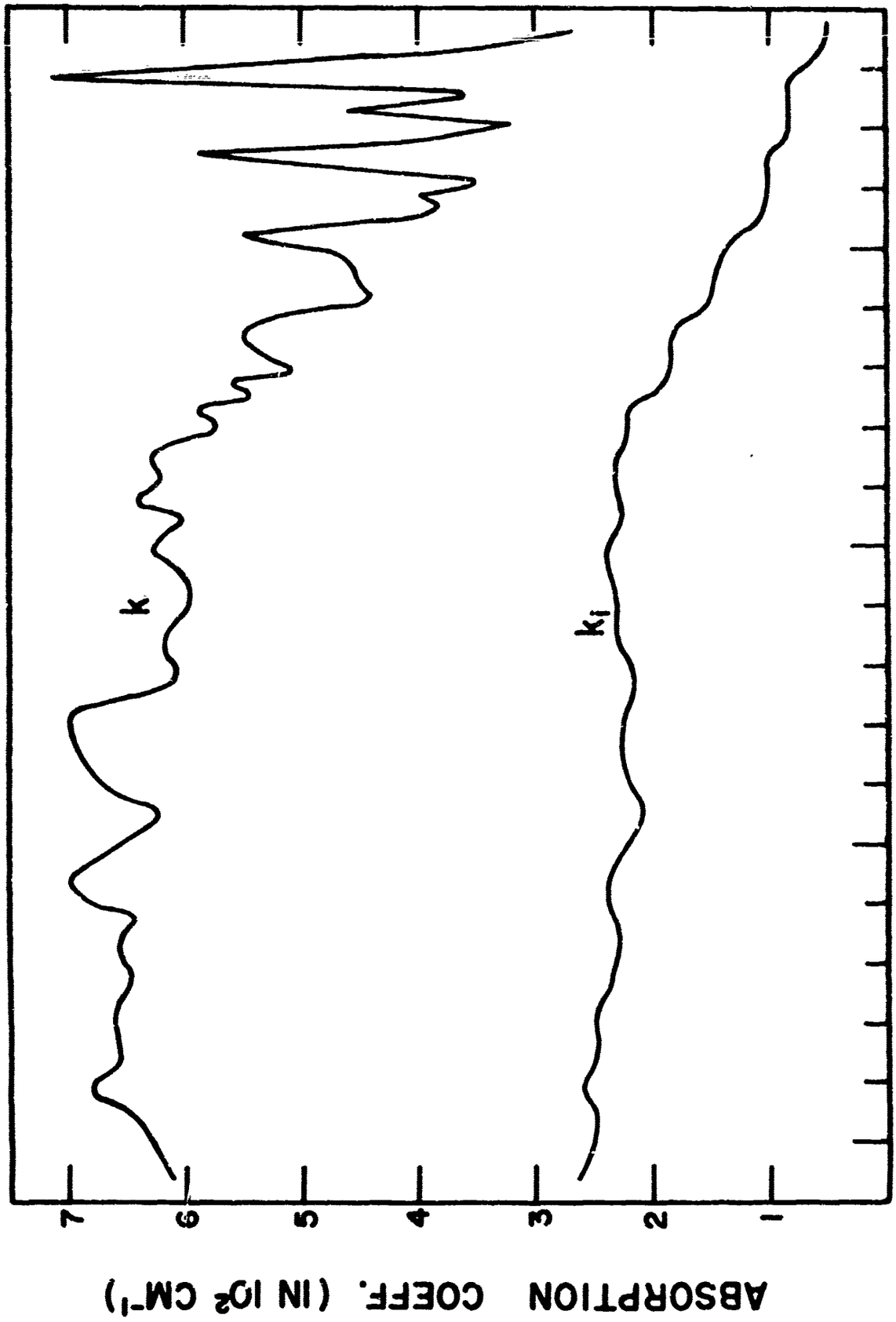

Figure 5. Absorption and photoionization coefficients of NH_3 in the 1000 - 1180 Å region

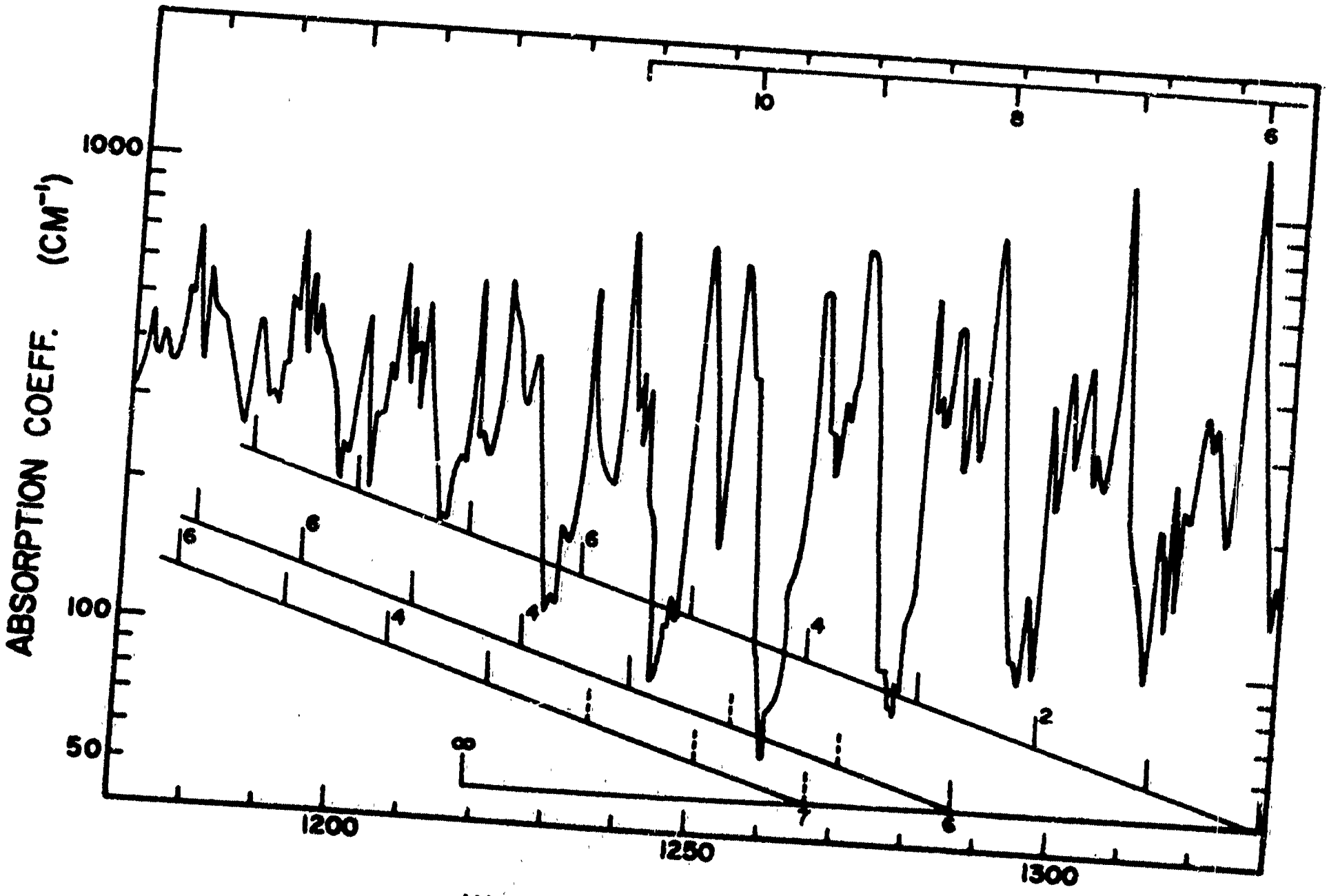

Figure 6. Absorption coefficient of NH_3 in the 1180 - 1330 Å region

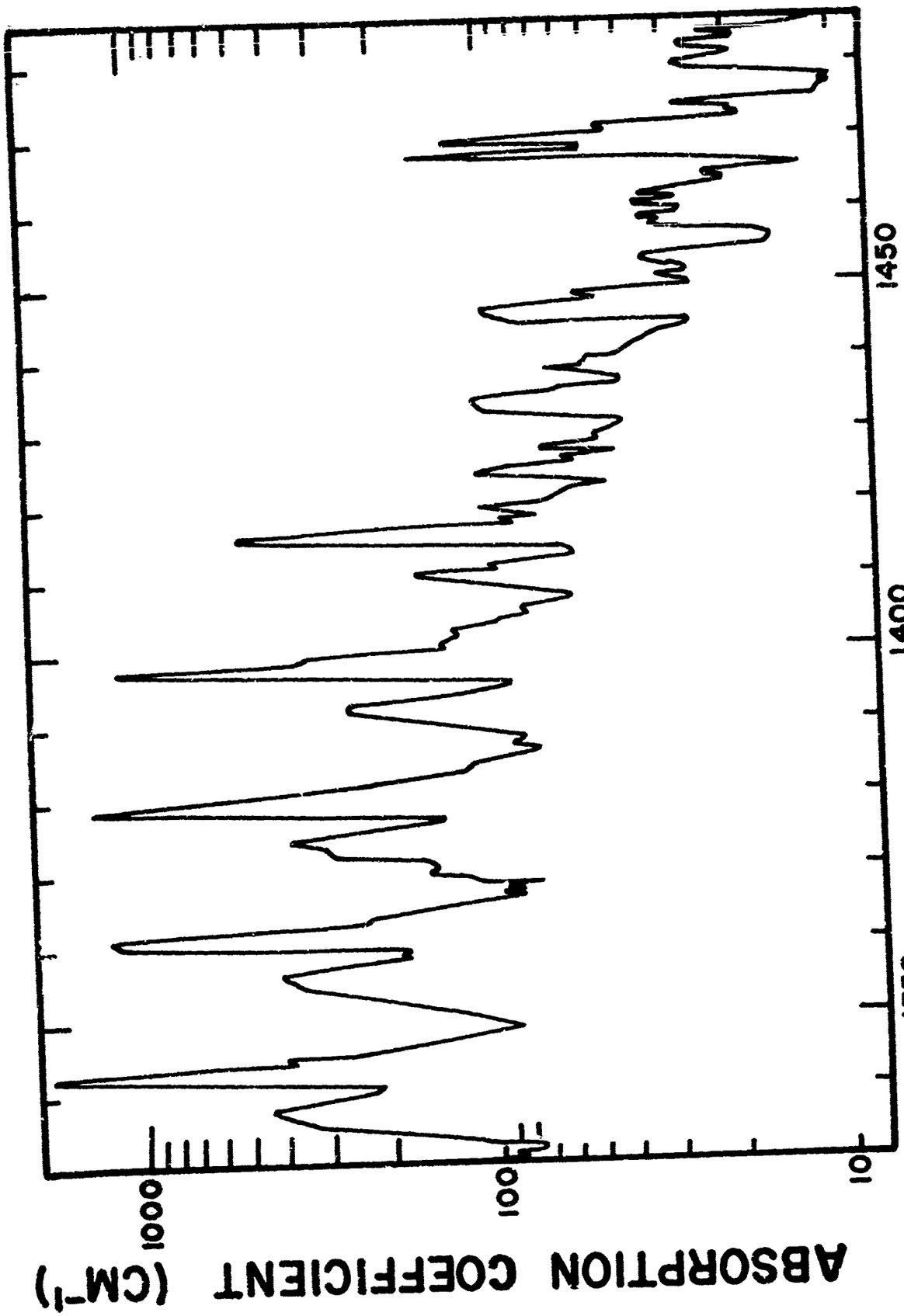

Figure 7. Absorption coefficient of NH_3 in the 1330 - 1480 A region

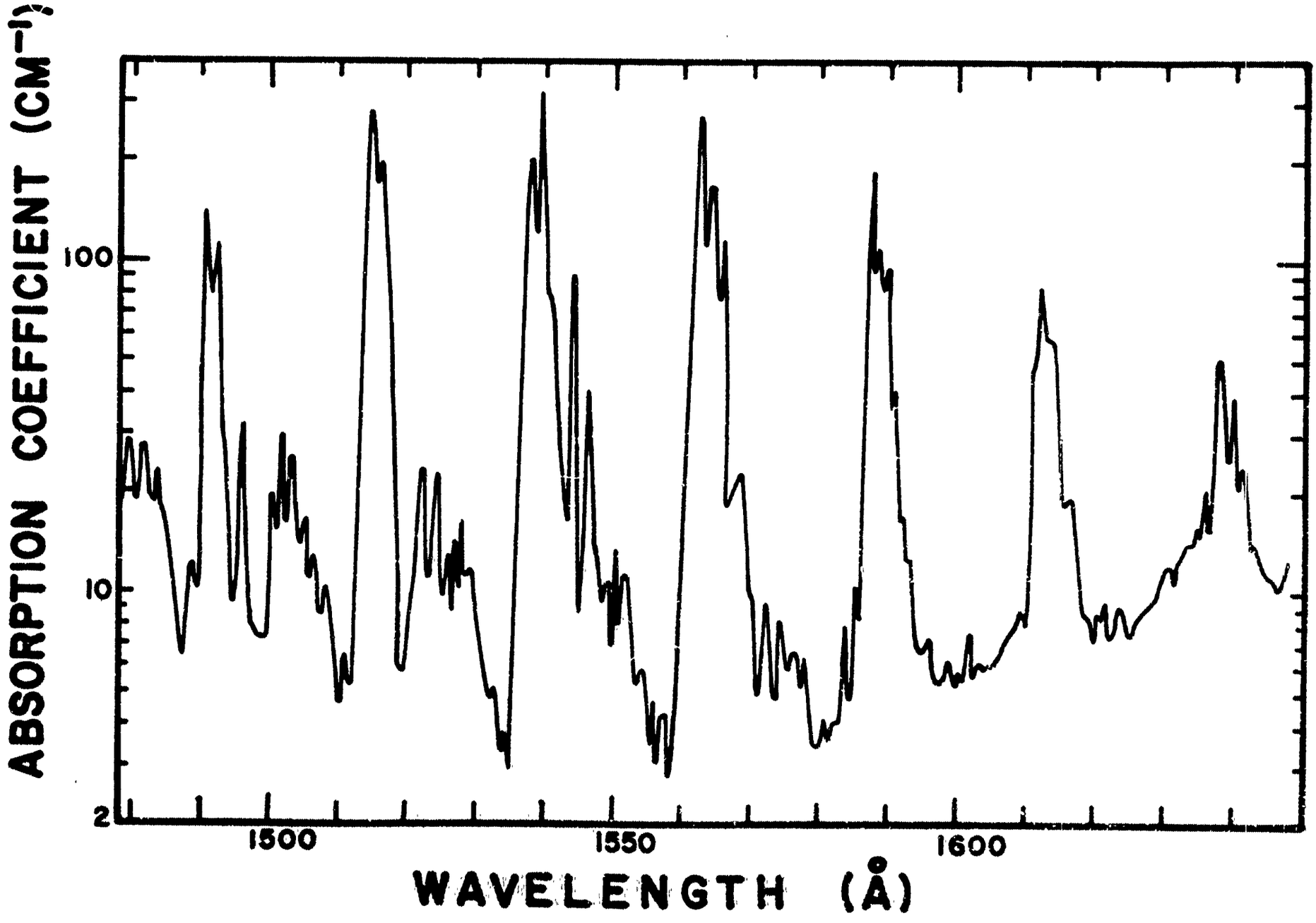

Figure 8. Absorption coefficient of NH_3 in the 1480 - 1650 A region

Table I. Absorption Coefficient k (in cm^{-1}) of NH_3 in the Region 580 - 1650 Å

λ	k	λ	k	λ	k
582.4	740	730.9	890	913.8	490
84.9	770	35.9	880	16.0	500
98.7	750	43.7	920	18.3	460
600.4	740	47.0	920	20.7	450
02.7	800	52.6	900	23.4	440
10.0	760	65.3	890	27.5	430
11.7	770	76.0	900	30.5	440
15.6	840	85.6	890	32.2	420
19.1	800	805.2	860	34.7	420
20.0	830	15.5	860	36.6	430
25.0	810	26.1	830	40.7	420
26.8	830	33.2	800	43.6	420
29.7	810	34.4	770	45.0	420
35.0	820	45.8	750	48.7	420
40.0	830	55.6	720	50.3	460
41.3	840	58.6	700	53.7	460
44.6	840	65.9	680	55.7	460
47.9	850	75.8	650	58.1	470
50.0	870	85.6	640	62.4	490
55.0	850	87.5	630	65.1	470
61.9	830	90.7	580	68.7	500
65.0	850	93.0	580	72.5	520
71.4	850	95.4	610	76.5	540
81.1	880	97.6	560	80.2	560
87.4	900	900.3	540	83.0	580
91.8	890	02.5	560	86.9	600
701.4	930	05.8	550	89.1	610
12.8	920	08.2	540	91.1	610
18.5	930	09.7	540	93.7	610
23.4	920	11.8	500	97.6	630

λ	k	λ	k	λ	k
1001.3	620	1100.5	640	1163.8	480
04.8	640	02.1	620	66.1	590
06.9	670	04.4	600	66.8	450
09.4	690	05.8	620	68.9	360
13.8	650	07.3	640	69.7	370
16.4	660	10.6	620	0.6	320
19.3	660	12.3	620	72.0	400
24.0	660	15.0	630	72.4	460
27.1	640	17.6	610	74.3	420
30.2	650	19.0	570	75.9	360
33.6	660	21.3	580	77.4	520
35.5	650	23.7	590	78.3	710
37.2	640	25.8	540	80.5	570
39.9	690	27.6	560	81.3	510
44.1	700	29.0	510	82.0	460
47.1	680	32.8	540	83.1	380
50.1	650	35.3	550	84.3	310
54.8	620	37.5	540	85.6	270
56.8	640	39.5	500	86.5	400
58.8	670	41.8	440	87.1	450
62.0	680	44.3	450	87.8	420
65.1	690	46.5	450	88.3	380
68.5	700	48.6	460	89.4	320
71.4	700	50.0	510	90.3	300
75.3	620	50.8	540	91.5	370
79.3	600	52.1	550	91.9	510
81.5	620	53.7	500	92.8	710
84.6	620	54.0	470	93.3	480
87.7	600	54.7	420	93.7	380
90.0	590	57.3	380	94.6	580
94.6	600	59.7	400	95.7	490
97.9	620	61.3	350	97.7	350
99.5	630	62.3	410	99.4	212

λ	k	λ	k	λ	k
1200.2	251	1235.2	258	1268.6	360
01.8	440	36.4	228	70.6	470
02.6	470	38.0	780	71.4	770
03.9	291	38.4	620	72.0	720
05.0	294	40.4	390	72.9	420
06.7	410	41.9	253	73.5	294
07.5	620	43.5	86	74.1	194
08.9	480	44.4	88	75.8	96
09.2	380	45.9	112	77.5	77
10.7	510	47.4	174	78.1	86
11.4	400	48.9	670	79.6	136
12.8	254	49.3	740	81.2	540
14.8	177	49.8	590	81.6	610
15.7	231	50.5	450	82.9	380
16.0	242	50.9	259	83.2	320
17.4	370	52.1	164	84.3	520
17.7	580	53.1	320	85.5	260
19.0	275	53.7	540	86.5	420
19.9	245	54.3	700	86.9	320
21.1	320	54.8	600	87.4	276
21.5	590	55.7	450	88.4	470
22.5	530	56.8	390	89.4	840
23.6	360	57.9	149	90.3	500
25.6	390	58.8	100	91.1	300
26.1	410	59.9	67	92.6	120
28.3	139	61.9	80	94.8	91
29.0	116	62.9	137	95.6	145
30.1	122	63.8	163	96.3	95
30.9	177	64.7	380	96.9	185
32.1	184	65.7	611	97.3	380
33.2	510	66.1	400	98.2	219
33.6	580	67.2	310	98.9	370
34.2	410	67.8	243	99.8	420

λ	k	λ	k	λ	k
1300.2	400	1332.3	76	1368.0	81
01.7	330	33.8	157	68.9	109
02.3	450	35.9	340	70.1	146
02.9	340	37.9	450	71.2	150
03.5	251	38.6	390	72.0	232
03.9	298	39.9	239	73.5	295
04.3	277	40.9	214	74.2	380
05.0	245	41.7	610	75.3	275
05.7	350	42.3	1840	76.0	198
06.5	1020	43.3	1110	77.1	139
07.6	610	43.6	690	78.1	400
08.7	310	45.0	281	78.7	1390
09.8	164	46.9	137	78.9	1510
10.9	146	47.3	118	79.4	1060
11.8	96	49.1	87	80.1	630
12.8	136	50.6	114	81.3	310
13.5	208	52.5	184	82.6	188
14.3	124	53.5	229	84.0	121
14.7	263	54.6	360	85.3	91
15.4	142	55.5	370	86.1	81
15.9	184	56.1	410	87.4	85
16.6	231	57.3	295	89.8	122
19.0	370	58.5	178	91.0	186
20.2	350	59.1	177	92.0	255
21.3	249	59.8	544	92.5	262
22.3	192	60.2	900	93.1	200
23.3	340	60.7	1560	94.9	100
24.4	1390	61.1	1270	95.7	87
24.7	1280	61.4	1040	96.2	150
25.1	950	62.0	660	97.4	1180
27.6	206	64.0	225	97.9	500
29.1	131	65.6	121	99.0	330
31.1	90	67.6	84	99.8	189

λ	k	λ	k	λ	k
1400.9	139	1436.7	41	1467.7	157
02.7	125	37.6	46	68.4	53
04.2	95	38.5	67	69.1	130
05.6	81	39.3	51	69.8	101
07.3	58	40.3	43	70.9	46
08.6	97	40.9	40	71.5	47
09.8	138	43.4	32	72.7	18.1
10.4	161	45.2	84	73.8	18.8
10.7	147	46.1	102	74.2	28.1
11.8	102	47.4	48	75.4	11.0
12.8	58	49.2	46	77.6	10.0
14.2	63	50.2	26.8	78.8	22.0
14.8	168	50.8	32	79.3	27.4
15.2	362	51.0	26.2	79.6	28.4
15.8	510	52.3	28.1	80.3	18.9
16.3	253	52.8	37	81.0	22.2
17.5	93	53.9	31	81.6	27.4
18.2	96	55.0	15.4	82.3	22.1
19.4	101	56.3	15.8	82.8	19.5
20.1	81	57.4	34	83.5	23.3
22.1	56	58.3	32	85.4	13.4
23.0	56	59.0	32	87.7	6.3
24.1	108	59.6	27.2	89.1	11.0
24.7	106	60.0	29.4	90.0	15.1
25.4	86	60.8	37	90.4	140
26.6	61	61.1	28.6	91.7	53
27.7	69	62.0	35	92.2	100
28.9	48	62.8	26.4	92.6	104
30.0	49	63.8	20.0	93.8	25.9
32.6	79	65.2	16.0	95.2	8.7
33.0	100	65.5	14.7	95.5	30
34.1	109	67.0	15.9	97.4	8.0
35.1	65	67.2	31	99.5	7.1

λ	k	λ	k	λ	k
1500.4	19.3	1526.6	8.4	1548.4	6.6
01.0	15.2	27.2	13.9	49.2	9.6
01.5	23.3	27.6	9.6	50.1	12.7
02.0	29.7	27.9	15.7	50.5	7.7
02.4	16.0	78 4	10.8	51.6	11.0
02.8	20.3	29.6	10.5	52.0	10.6
03.7	20.4	30.8	6.0	53.3	4.5
04.3	13.9	31.3	5.9	53.7	5.6
04.8	15.6	32.4	4.6	55.0	3.5
05.7	10.9	34.2	3.0	55.9	4.5
06.5	12.7	34.9	2.4	56.5	2.9
07.7	8.5	36.4	11.1	57.6	3.7
08.3	10.3	36.6	8.2	58.3	2.6
09.6	5.6	36.8	14.6	58.8	2.7
10.7	4.2	37.0	11.5	59.3	4.3
11.3	7.2	37.2	23.8	60.4	5.8
12.0	5.6	37.5	117	61.2	7.0
12.5	12.2	38.4	197	62.5	260
13.4	54	38.9	115	63.2	120
13.9	75	39.4	285	64.1	164
14.5	198	40.1	78	64.9	102
15.0	269	41.0	71	65.3	75
15.9	166	41.8	53	65.8	115
16.2	192	42.3	16.9	66.3	71
17.5	70	42.7	21.8	68.7	21.8
18.7	14.7	43.1	17.3	69.5	10.0
19.9	5.5	43.6	13.8	71.4	5.1
20.4	7.7	44.1	42	72.3	9.4
22.3	23.4	44.6	20.7	72.6	7.2
23.2	11.1	44.9	8.5	73.4	4.7
24.2	22.8	45.9	9.7	74.3	6.9
25.8	9.7	46.7	52	74.7	8.2
26.0	13.1	47.1	14.6	75.8	5.8

λ	k	λ	k	λ	k
1576.4	6.6	1600.3	5.8	1632.7	12.8
77.4	5.2	01.7	5.4	33.6	13.9
77.7	6.3	02.0	7.5	34.1	14.1
78.5	4.7	02.4	5.6	35.2	16.6
79.2	3.4	02.8	5.9	36.3	25.3
80.0	3.8	03.1	6.1	37.7	77
81.1	4.2	04.5	6.0	38.1	81
81.4	3.5	05.2	6.0	38.4	33
82.4	4.0	06.2	6.4	38.9	29
83.9	8.0	07.0	7.2	39.3	40
84.4	4.8	08.4	7.8	39.5	48
85.0	7.9	09.0	8.3	40.3	20.9
85.4	11.8	09.6	8.6	41.5	20.8
86.1	8.1	10.3	9.6	42.9	13.6
86.7	62	10.9	47	43.6	14.1
87.4	188	11.7	83	44.4	11.5
87.8	93	12.4	69	45.6	11.1
88.2	109	13.7	57	46.0	10.3
88.8	81	14.8	41	47.9	11.7
89.0	96	15.5	25.4		
89.2	62	16.7	23.7		
90.8	24	17.6	13.0		
91.3	37	18.5	8.5		
92.3	17.4	19.8	7.1		
92.9	12.5	20.1	7.5		
93.8	10.1	20.8	8.1		
94.8	6.5	21.1	7.3		
95.3	6.6	21.9	7.3		
96.1	7.3	23.5	7.7		
97.0	5.3	25.7	8.0		
98.3	5.5	29.8	11.1		
98.8	6.3	30.5	12.0		
99.9	5.2	31.2	10.8		

Table II. Wave Numbers of Band Progressions in cm^{-1}

1434 A transition

n'	Walsh	This work	
0	69758	69759	
			878
1	70644	70637	
			925
2	71569	71562	
			954
3	72516	72516	
			970
4	73498	73486	
			1002
5	74497	74488	
			1012
6	75508	75500	
			1040
7	76545	76540	
			1034
8	77590	77574	
			1066
9	78649	78640	
			1073
10		79713	
			1056
11		80769	

1330 A transition

Walsh	This work	
75212	75216	
		922
76133	76138	
		945
77064	77083	
		951
78045	78034	
		974
79031	79008	
		1031
80042	80039	
		1025
81072	81064	
		1058
82098	82122	
		1066
	83188	
		1051
	84239	
		1063
	85302	

1287 A transition

	Duncan	This work	
0		(77715)	
			930
1		(78645)	
			955
2		(79600)	
			980
3	80618	80580	
			999
4	81597	81579	
			1018
5	82606	82597	
			1036
6	83600	83633	
			1055
7	84749	84688	
			1068
8	85769	85756	
			1065
9	86839	86821	

1266 A transition

Duncan	This work	
78931	(78940)	
		940
	(79880)	
		960
80832	(80840)	
		980
81884	81820	
		996
82857	82816	
		1020
83843	83836	
		1039
84872	84875	
		1050
85928	85925	

decreases to about 20 %/o at 1175 A. The lower curve in Fig. 5 shows the photoionization coefficient k_i. Since this curve does not show the band structure appearing in the upper curve, we conclude that the bands are not preionized and their diffuseness is probably due to predissociation. The difference between the two curves indicates that dissociation is the predominant process for this region. The peak of the broad dissociation continuum appears to be at about 1060 A. The steps in the k_i-curve which appear in the region above 1120 A are interpreted as vibrational structure in the ionization continuum corresponding to transitions to vibrationally excited NH_3^+ ion. These steps form an extension of our previous result[7] for the region 1160-1230 A. The positions of the steps for the overlapping region are in good agreement and the $\Delta\nu$ of the steps is consistent with the vibrational $\Delta\nu$ of the Rydberg bands discussed in the next section.

The k-values for this region are about 10 %/o higher than our earlier values[6] obtained with lower resolution. About half of the measured mean k-values for this region are listed in Table I. The present ionization efficiencies are on the average about 10 %/o lower than those reported earlier;[6] however, the new result is based on more reliable yield data of NO and is consistent with shorter wavelength data obtained with xenon as a reference gas.

c. 1180-1480 A Region

Ammonia has a very complex spectrum in this region. The general feature of this spectrum can be attributed to electronic

transitions involving the change of configuration from the pyramidal ground state to planar excited states. Experimental evidences for the planar state were obtained by Walsh and Warsop[8] and Douglas and Hollas.[9] Earlier studies[3,6] have suggested the large change of configuration. This change involves the ν_2 frequency (~900 cm^{-1}) corresponding to the normal mode vibration in which the height of the pyramid changes. These interpretations are consistent with the presence of several long progressions involving this frequency. The 0-0 transition is non-vertical and the present study shows that strongest bands in each progression is $v' = 5$ or 6.

The k-value for this region is shown in Figs. 6 and 7, which use semi-log scale, and about half of the mean k-values are also listed in Table I. The k-values range from 10 to 1800 cm^{-1} and are probably more reliable than those obtained previously;[6] the maxima are higher and minima are lower as they should be with improved resolution. Furthermore, many more structures were resolved. Despite these improvements, the k-values at some of the strongest bands showed significant pressure dependence which can be ascribed to insufficient resolution. Further measurements with continuous background and higher dispersion are needed to obtain quantitative k-values for the sharp bands.

Walsh and Warsop[8] have used the 0-0 band of the 1330 A and 1434 A progressions to obtain the Rydberg series:

$$\nu = 82150 - R/(n-1.024)^2 \qquad n = 4,5$$

The ionization limit 10.18 eV is in good agreement with the photoionization value[7], but it is desirable to identify

additional members of this series. For this purpose, four progressions are listed in Table II. The 1434 A transition is Duncan's Series III but the wave numbers by Walsh and Warsop are used here because they agree somewhat better with our results. The bands with n' = 10 and 11 were also observed by Duncan. The 1330 A transition was proposed by Walsh and Warsop. All the bands in this transition including those with n' = 8,9 and 10 appear in Duncan's table of sub-bands.[3] The remaining two transitions in Table II are proposed in this work and are discussed below.

Figs. 6 and 7 show that the 5-0 and 6-0 bands are the strongest bands in the 1434 A transition and the 5-0 band is the strongest in the 1330 A progression. Walsh and Warsop estimated the strongest band to be the 4-0 band in both progressions.

The existence of the two proposed transition (1287 A and 1266 A in Table II) is strongly supported by Duncan's table of sub-bands. Differences of 50 cm^{-1} in the observed wave numbers is quite possible since we have used the H_2 source and 0.2 A resolution. Values in parentheses were obtained by extrapolation with $\Delta\nu$ = 930-980 cm^{-1}. The justification for this extrapolation is as follows: (a) the extrapolated bands of both progressions are expected to be very weak and their estimated positions (see Fig. 6) lie close to the strong heads of the 1434 A progression, thus making identification difficult; (b) the strongest bands of both transitions are the 6-0 bands and the intensity distribution of these transitions is consistent with those of the 1330 A and 1434 A

transitions; (c) the $\Delta\nu$ between the successive bands is consistent with the trend shown in the 1330 A and 1434 A transitions. Thus the two proposed transitions appear to be electronic transitions of the Rydberg type. It should be noted that the present 1287 A transition is different from the 1286 A transition of Walsh and Warsop; although the origins are nearly the same, the bands are different and the $\Delta\nu$ in the present case is more consistent with the other progressions. If our inferences are correct, some 13 unclassified bands, most of which are quite prominent in the region below 1300 A, become classified.

The wave number of the 0-0 band of the four transitions listed in Table II approximately fits the series

$$\nu = 82000 - R/(n-0.97)^2 \qquad n = 4,5,6,7$$

The differences between the calculated and observed or extrapolated wave numbers are 288, 27, -52 and 42 cm^{-1} for the four bands taken in the order of increasing n. The above equation supports the series formula by Walsh and Warsop. The convergence limit 82000 cm^{-1} corresponds to 10.166 eV which is close to the photoionization value 10.154 eV.[7]

According to Walsh and Warsop, the electron excited in the upper state of the 2168 A - 1434 A - 1330 A Rydberg transition is the ns type and they formulated the following transition:

$$(a_1')^2\ (e')\ (a_2'')\ (nsa_1'),\ {}^1A_2'' \leftarrow (a_1)^2(e)^4(a_1),{}^1A_1\ (n=3,4,5)$$

The present study suggests that the 1287 A and 1266 A transitions belong to this system with n=6 and 7.

d. 1480-1650 A Region

Fig. 8 shows the absorption coefficient of NH_3 for this region in semi-log scale. The k-values vary from 2.6 to 285 cm^{-1} and are consistent with our earlier results which showed k-values from 3.4 cm^{-1} at the deepest valley and 220 cm^{-1} at the peak of the strongest band.

According to Douglas and Hollas[9] the origin of the progression of the bands in this region is at about 1689 A. On the basis of the new origin, Fig. 8 shows that the 6-0 is the strongest band of the 1689 A progression. According to Walsh and Warsop[8] this progression is the first member of a Rydberg series involving the np type orbital in the excited state. The present work shows that the intensity of this progression of bands is nearly one order of magnitude lower than the 1434 A progression; however, it appears to be strong enough to be interpreted as an allowed transition. In view of the weakness of the second Rydberg series, higher members are probably overshadowed by members of the first series.

REFERENCES

1. S. W. Leifson, Astrophys. J. 63, 73 (1926).
2. J. K. Dixon, Phys. Rev. 43, 711 (1933).
3. A. B. F. Duncan, Phys. Rev. 47, 822 (1935).
4. A. B. F. Duncan, Phys. Rev. 50, 700 (1936).
5. A. B. F. Duncan and G. R. Harrison, Phys. Rev. 49, 211 (1936).
6. K. Watanabe, J. Chem. Phys. 22, 1564 (1954).
7. K. Watanabe and J. R. Mottl, J. Chem. Phys. 26, 1773 (1957).
8. A. D. Walsh and P. A. Warsop, Trans. Faraday Soc. 57, 345 (1961).
9. A. E. Douglas and J. M. Hollas, Can. J. Phys. 39, 479 (1961).
10. R. J. Thompson and A. B. F. Duncan, J. Chem. Phys. 14, 573 (1946).
11. E. Tannenbaum, E. M. Coffin, and A. J. Harrison, J. Chem. Phys. 21, 311 (1953).
12. K. Watanabe, M. Zelikoff, and E. C. Y. Inn, Geophysical Research Paper, No. 21, Air Force Cambridge Research Laboratory (1953).
13. H. Sun and G. L. Weissler, J. Chem. Phys. 23, 1160 (1955).
14. P. H. Metzger and G. R. Cook, J. Chem. Phys. 41, 642 (1964).
15. W. C. Walker and G. L. Weissler, J. Chem. Phys. 23, 1540 (1955).

16. K. Watanabe and J. R. Mottl, Threshold of Space, edited by M. Zelikoff (Pergamon Press, London, 1957) p. 151.

17. R. Onaka, Science of Light 7, 23 (1958).

18. F. S. Johnson, K. Watanabe, and R. Tousey, J. Opt. Soc. Am. 41, 702 (1951).

19. J. J. Hopfield, Phys. Rev. 35, 1130 (1930); 36, 784 (1930).

20. R. E. Huffman, Y. Tanaka, and J. C. Larrabee, J. Opt. Soc. Am. 52, 851 (1962).

21. R. G. Newberg, L. Heroux, and H. E. Hinteregger, Appl. Opt. 1, 733 (1962).

22. R. E. Huffman, Y. Tanaka, and J. C. Larrabee, Appl. Opt. 2, 617 (1963).

23. G. R. Cook and P. H. Metzger, J. Chem. Phys. 41, 321 (1964).

24. P. H. Metzger and G. R. Cook, J. Quant. Spectry. Radiative Transfer 4, 107 (1964).

25. F. M. Matsunaga, R. S. Jackson, and K. Watanabe, J. Quant. Spectry. Radiative Transfer (in press).

26. K. Watanabe, E. C. Y. Inn, and M. Zelikoff, J. Chem. Phys. 21, 1026 (1953).

27. K. Watanabe and F. F. Marmo, J. Chem. Phys. 25, 965 (1956).

28. K. Watanabe and F. M. Matsunaga, unpublished material.

29. J. A. R. Samson, J. Opt. Soc. Am. 54, 6 (1964).

30. R. E. Huffman, Y. Tanaka, and J. C. Larrabee, Discussion Faraday Soc. 37, 159 (1964).

31. R. E. Huffman, Y. Tanaka, and J. C. Larrabee, J. Chem. Phys. 39, 910 (1963).

III

ABSORPTION AND PHOTOIONIZATION COEFFICIENTS OF CO_2 IN THE REGION 580-1670 A

By R. S. Nakata, K. Watanabe, and G. M. Gnanapragasam

1. INTRODUCTION

The absorption spectrum of CO_2 in the vacuum ultraviolet region has been studied by a number of investigators. Early studies were made by Lyman,[1] Leifson,[2] Henning,[3] Rathenau,[4] and Price and Simpson.[5] Henning[3] discovered a doublet series converging to the limit 18.07 eV and two progressions, each with a band interval of about 1100 cm^{-1}. Rathenau[4] confirmed these findings and observed five non-Rydberg progressions in the region 900-1170 A. Mulliken[6] predicted the first ionization potential to be at 13.78 eV by assuming that the 2900 A emission band corresponds to the transition $^2\Sigma_u^+ \rightarrow {}^2\Pi_g$ of CO_2^+ and that Henning's series limit is the upper state. His prediction was confirmed by Price and Simpson[4] who identified an intense Rydberg series converging to 13.79 eV and two weaker series converging to the same limit. They also corrected the n=3 member of Henning's Rydberg series.

Recently, Tanaka, Jursa, and LeBlanc,[7] using the helium and argon continuum sources, reinvestigated the region 600-1650 A. They confirmed most of the earlier results and discovered several new Rydberg series and other progressions. Three of the Rydberg series converge to 19.38 eV which apparently corresponds to the $^2\Sigma_g^+$ state of CO_2^+. They also observed two vibrational Rydberg series, one associated

with Henning's series and the other with the series of Price and Simpson. They were able to resolve the doublet ionization limits, 13.787 eV and 13.765 eV, predicted by Mulliken.[6] Later, Tanaka and Ogawa,[8] using a 6.8-m grazing incidence spectrograph, discovered sixteen new Rydberg series converging to the v'=0 to v'=7 levels of the doublet $^2\Pi_u$ state of CO_2^+ predicted by Mulliken[6] and established the v'=0 levels of $^2\Pi_u$ state to be 17.312 eV and 17.323 eV above the ground state CO_2. Thus four electronic states of CO_2^+ have been determined, but there remain many unidentified CO_2 bands in the region above 900 A.

Most of the observed vibrational bands have $\Delta\nu$ in the range 1100-1350 cm^{-1} which apparently corresponds to the ν_1 symmetry frequency of the ground state of CO_2.

The absorption coefficient of CO_2 has been measured by several investigators: Wilkinson and Johnston[9] (1440-1670 A), Inn, Watanabe, and Zelikoff[10] (1050-1750 A) and Sun and Weissler[11] (370-1310 A). Wilkinson and Johnston reported a continuum with a maximum at 1495 A and three bands at 1662, 1673, and 1690 A. Inn et al observed a maximum at 1475 A and numerous diffuse bands in the 1400-1650 A region. They also reported two other continua with peaks at 1121 and 1332 A and bands superposed on these continua. Sun and Weissler observed a continuum below 860 A which was interpreted as the ionization continuum, but their light source was inadequate to provide a detailed profile of absorption bands. Wainfan, Walker, and Weissler[12] obtained photoionization cross sections at about thirty wavelengths in the region

450-800 A.

The present work consists of (a) a remeasurement of absorption coefficient in the region above 1000 A with improved resolution of 0.2 A to obtain more quantitative k-values at band centers and to resolve the long wavelength bands, (b) similar measurements in the region 580-1000 A, using the Hopfield continuum and 0.3 A resolution to obtain a more detailed spectrum, and (c) measurements of ionization efficiencies in the region 580-905 A.

2. EXPERIMENTAL

The apparatus and experimental procedures used for the study of CO_2 absorption are described in Part II.

The gas samples were drawn from reagent grade CO_2 obtained from Matheson Company in one liter flasks. Gas pressures and cell lengths used for the determination of absorption coefficient were as follows: 0.006 to 102 mm Hg in a 10.5 cm cell with LiF windows for the region 1060-1675 A, 0.006 to 0.120 mm Hg in windowless cells of 13.6 and 27.1 cm for the region 850-1100 A, and 0.010 to 0.150 mm Hg in a 11.5 cm cell for the region 580-1010 A. The helium continuum source was used for the last region, while the H_2 source was used for the longer wavelength region. Pressures from 0.02 to 0.15 mm Hg in a 54 cm cell were used for photoionization measurements.

The agreement of the results obtained with the static and flow type cells in the overlapping region 1060-1100 A indicated that our pressure measurements were reliable for

the case of windowless cells. The experimental error in the k-value determination for diffuse bands and continuum was estimated to be about 10 %. In the region below 670 A, where the source intensity was low, the error was estimated to be 15-20 %. In the regions 700-790 A and 900-1000 A, where there are a number of sharp bands, the k-values at some of the band peaks showed considerable pressure dependency, which was ascribed to incomplete resolution. In these cases, the k-values obtained with the lowest two or three pressures were used to obtain a mean k-value. Even so, the k-value at the sharpest bands may be too low. The experimental error in the determination of ionization efficiency was about 10 % so that the combined error in the k_1-values ranged from 15 to 30 %.

3. RESULTS AND DISCUSSION

a. 580-780 A Region

Mean absorption coefficients of CO_2 in this region are summarized by the k-curve in Fig. 9 and some of the values are listed in Table III. The spectrum shown in Fig. 9 is consistent with the photographs presented by Tanaka *et al.*[7,8] Essentially all the bands appearing in our figure have been identified by them, and their high-resolution study[8] has revealed many more Rydberg bands which were not resolved in the present study.

The k-values reported by Sun and Weissler[11] are shown by x in Fig. 9. In the region 580-680 A, where the Rydberg series[7] are extremely weak, the absorption is mainly due to

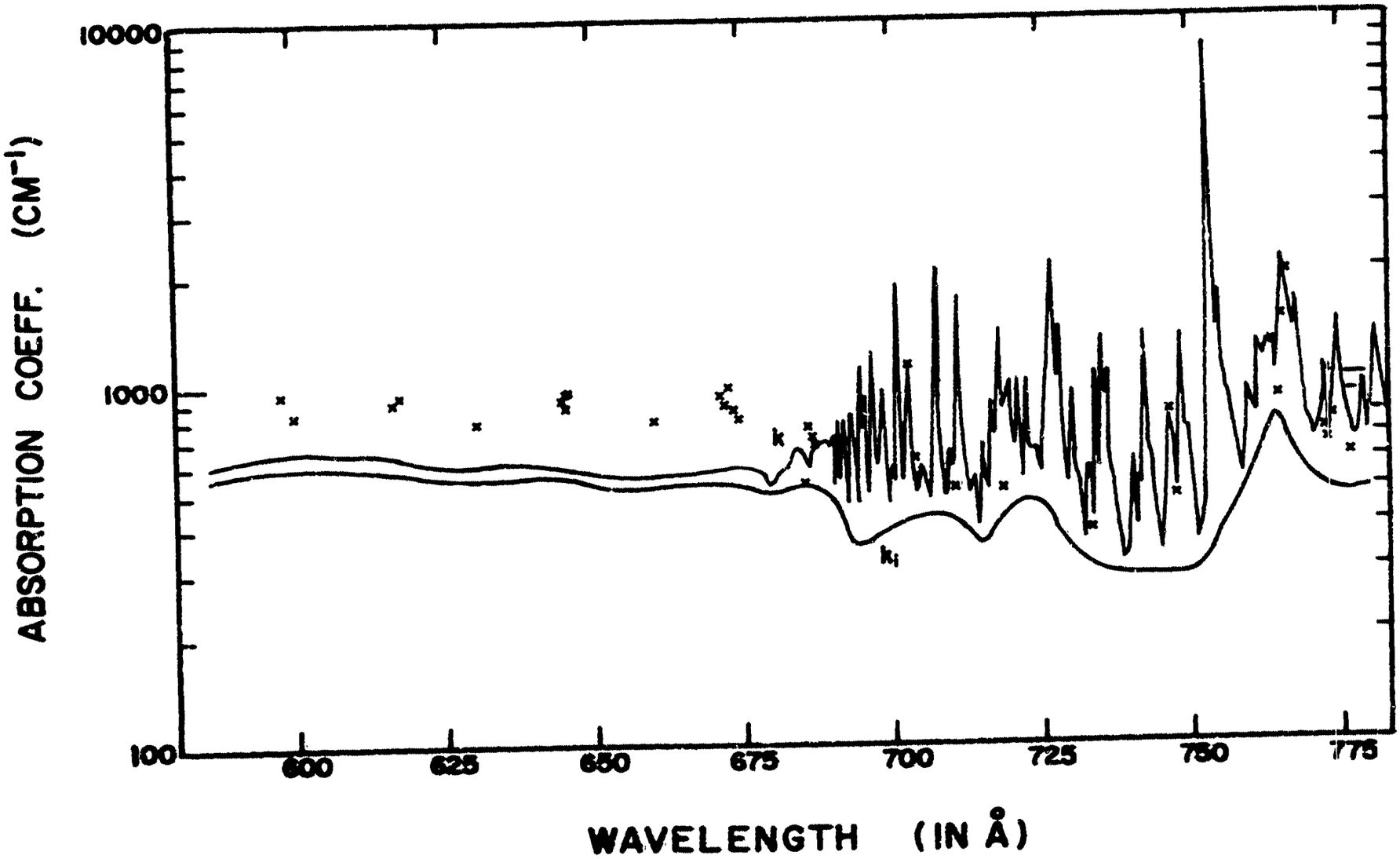

Figure 9. Absorption and photoionization coefficients of CO_2 in the region 580 - 780 A. x's are values by Sun and Weissler

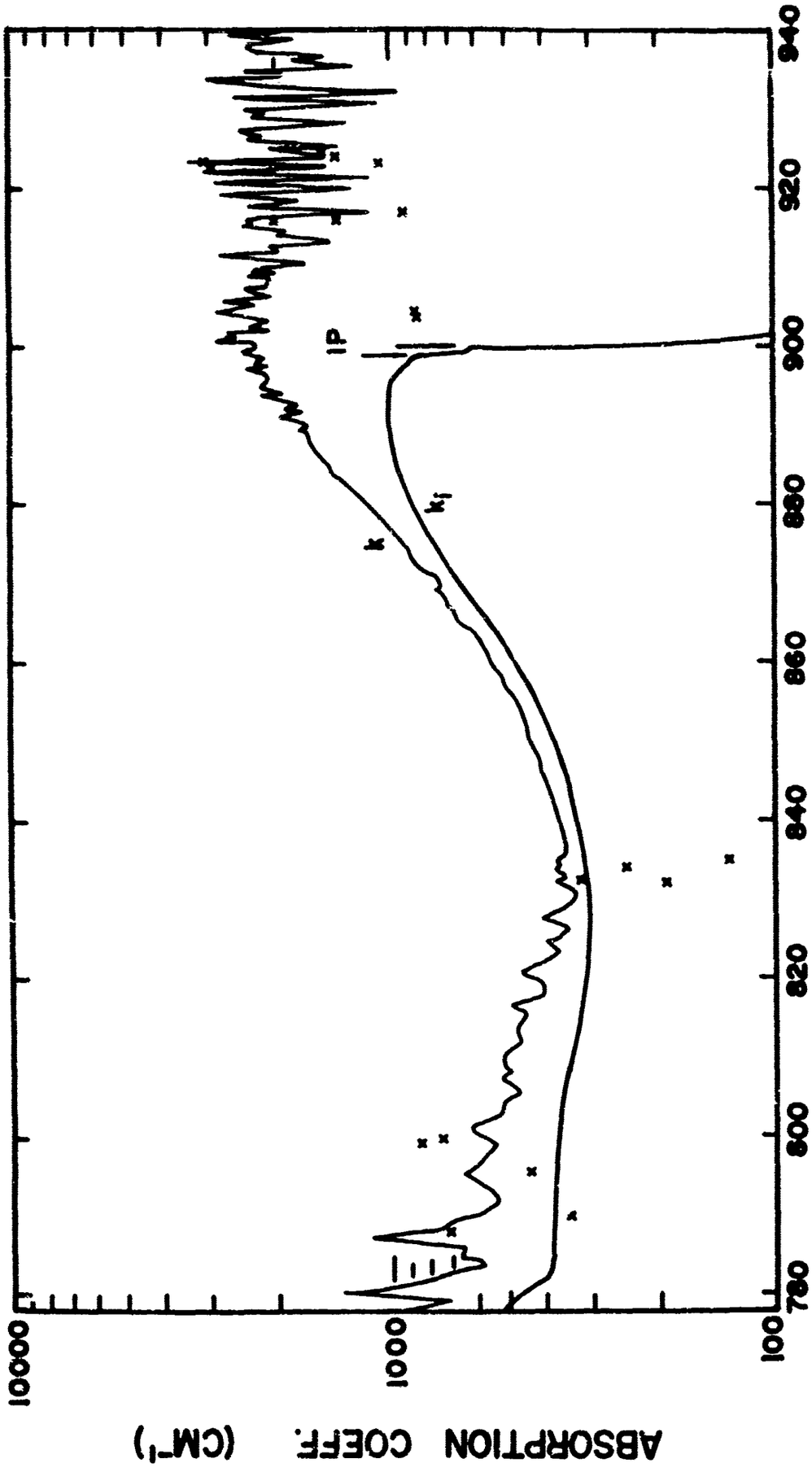

Figure 10. Absorption and photoionization coefficients of CO_2 in the region 780 - 940 A. x's are values by Sun and Weissler

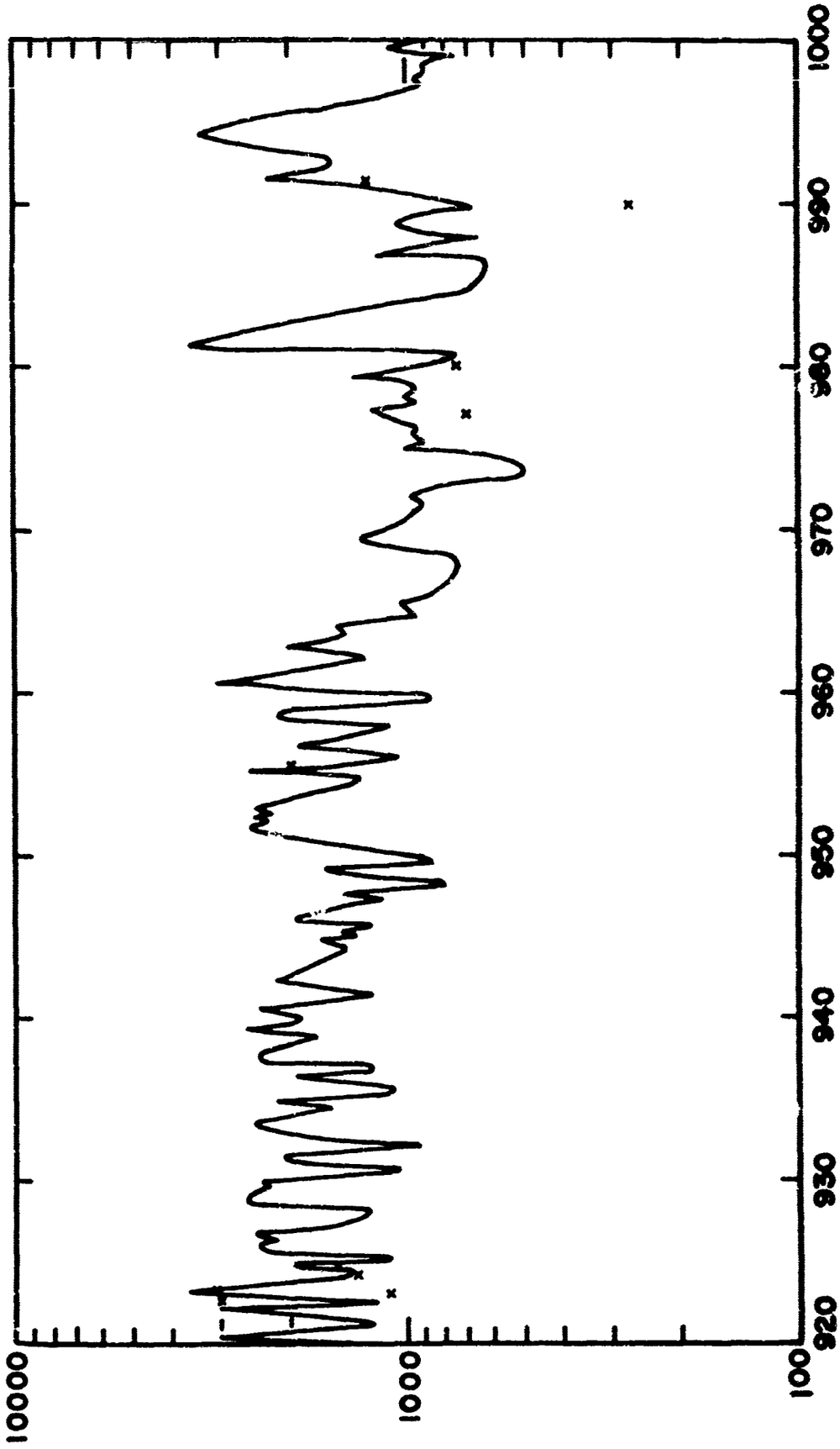

Figure 11. Absorption coefficient of CO_2 from 920 to 1000 Å

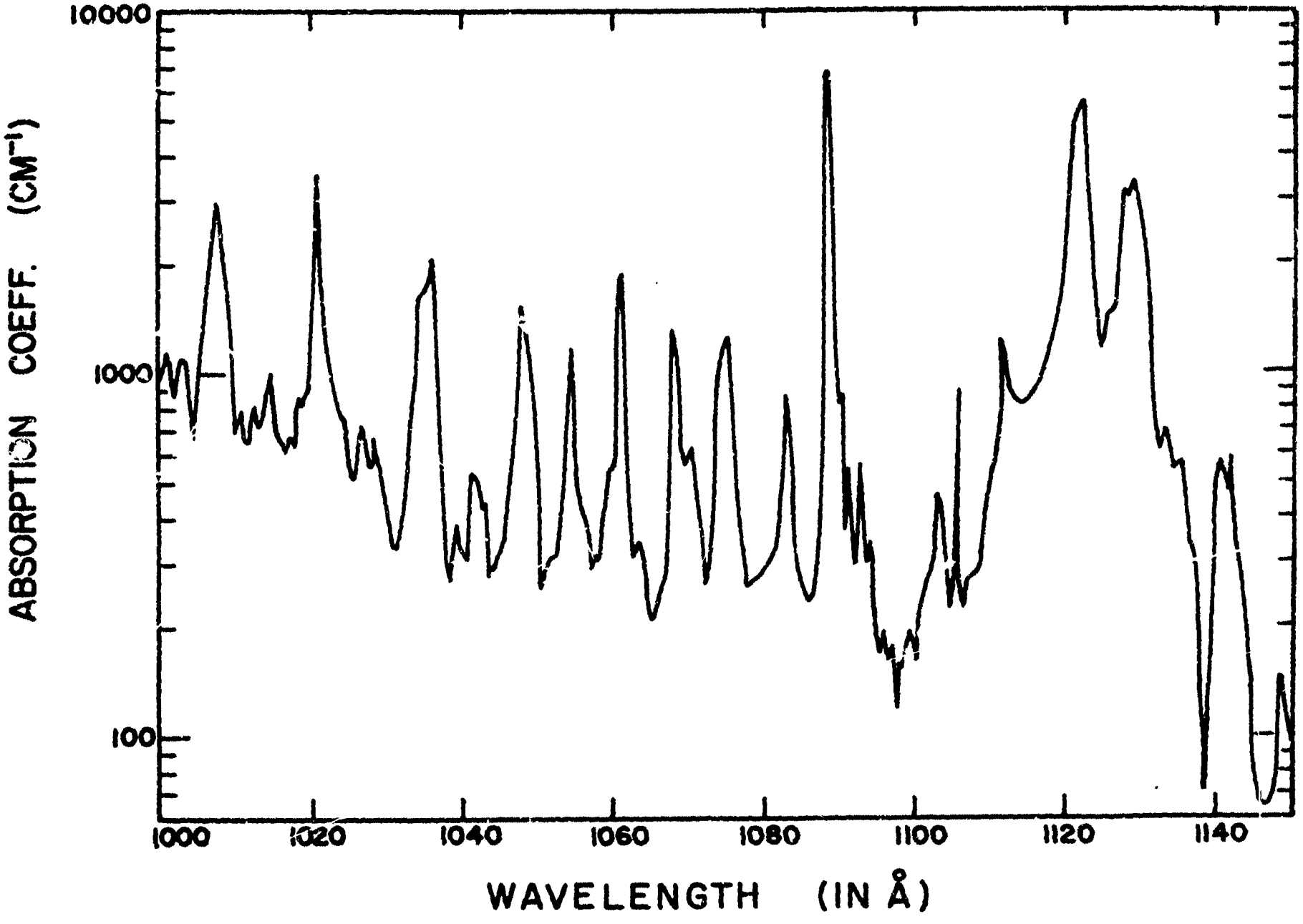

Figure 12. Absorption coefficient of CO_2 from 1000 to 1150 A

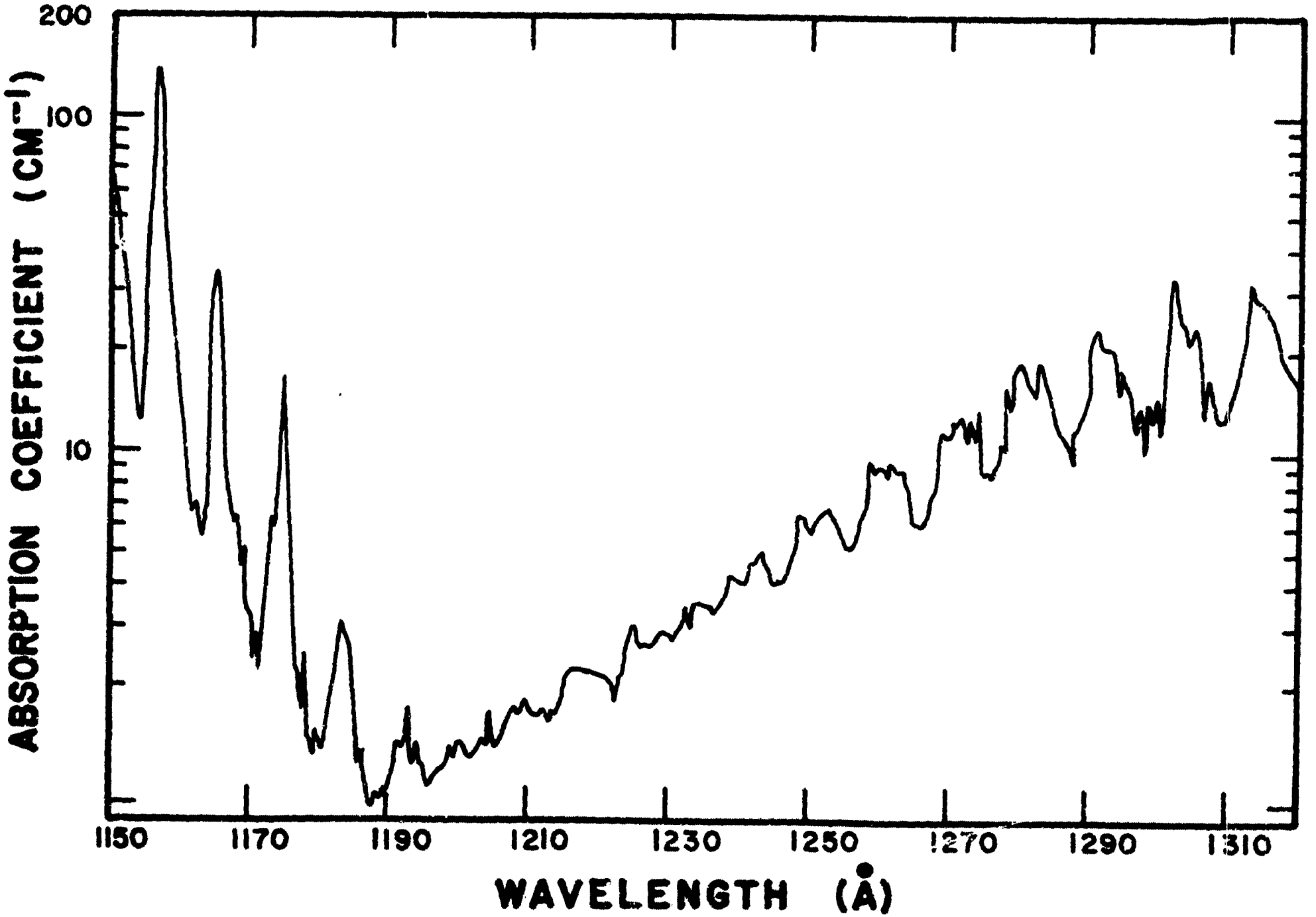

Figure 13. Absorption coefficient of CO_2 from 1150 to 1320 A

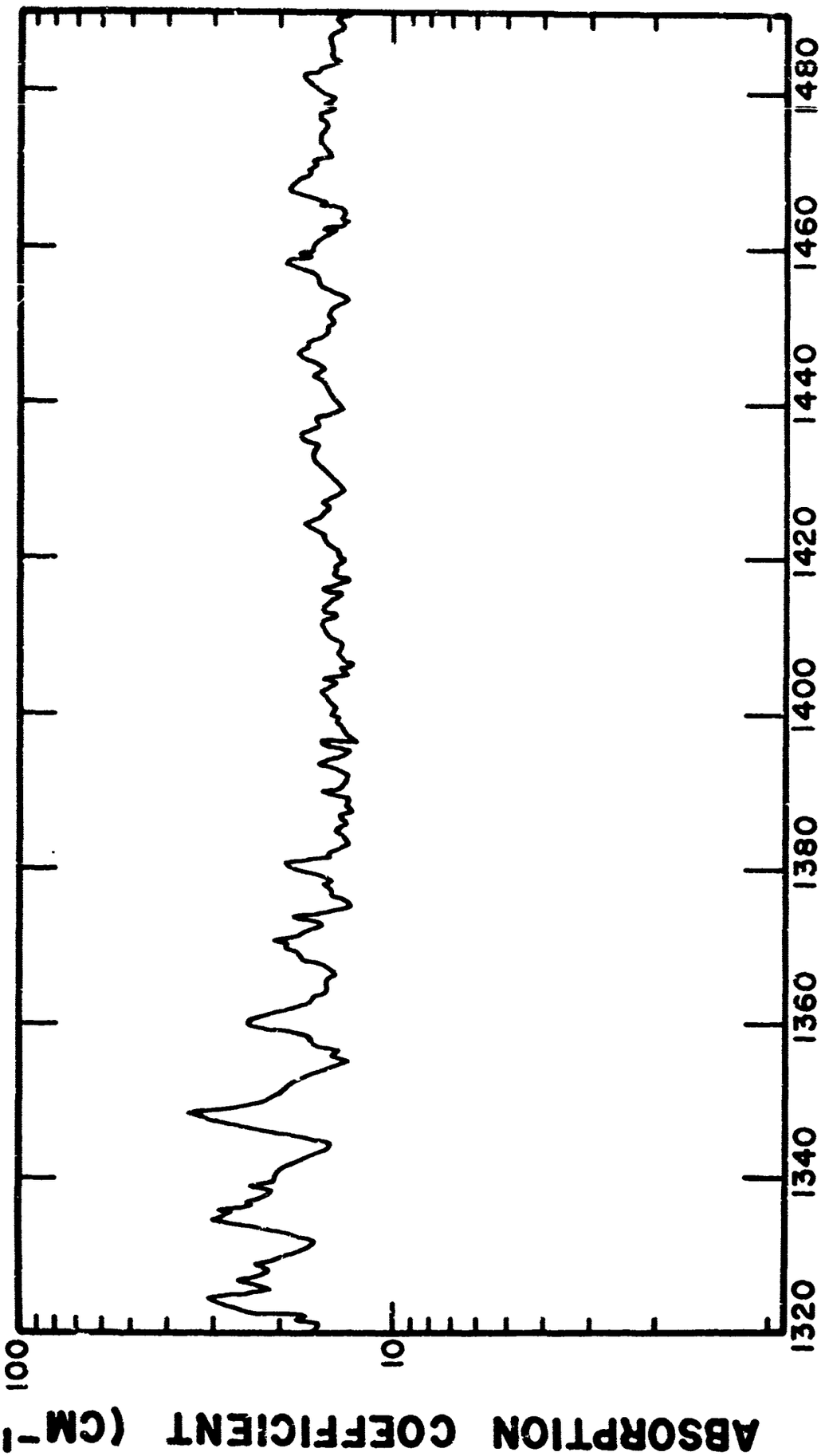

Figure 14. Absorption coefficient of CO_2 from 1320 to 1490 A

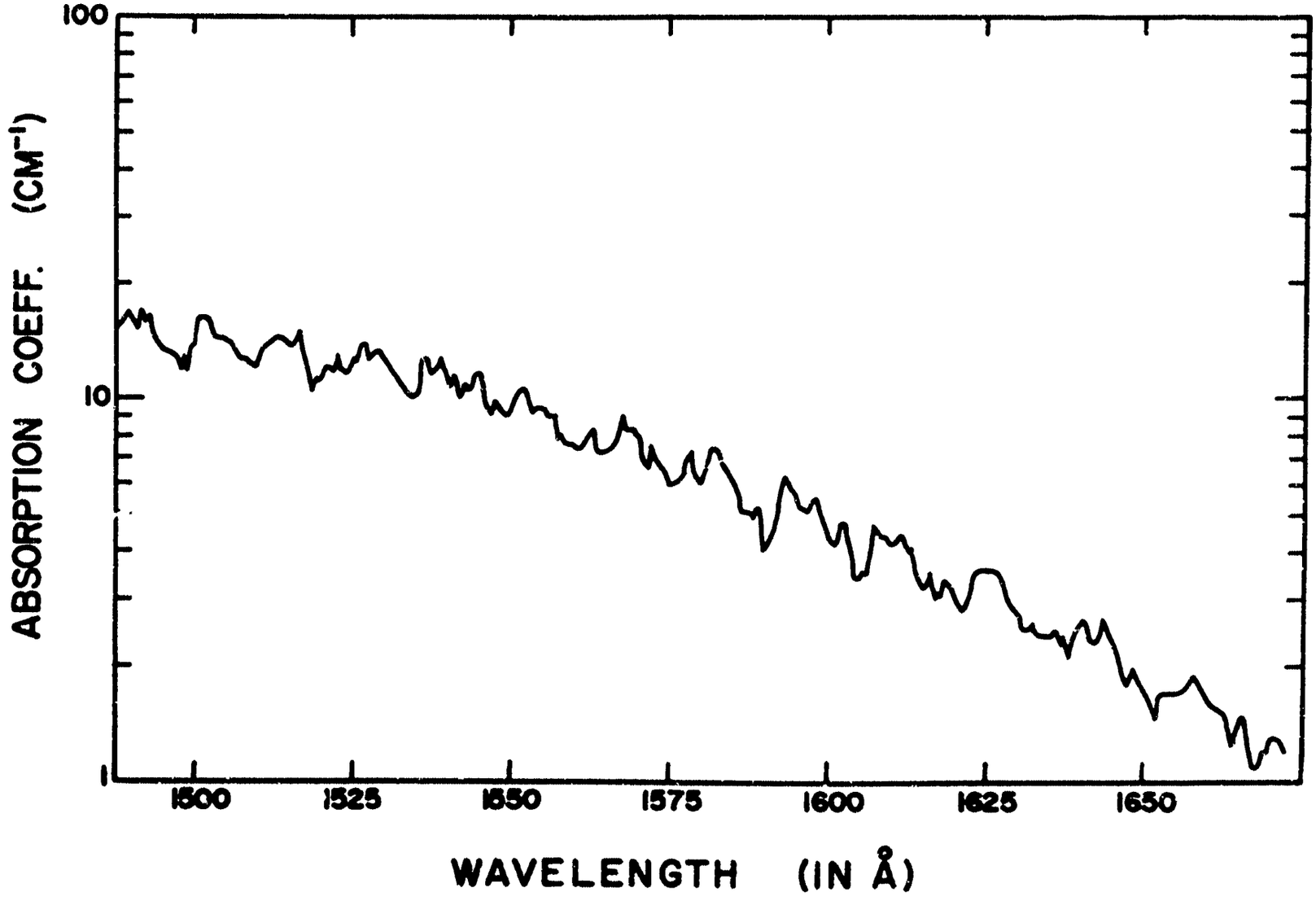

Figure 15. Absorption coefficient of CO_2 from 1490 to 1670 A

Table III. Absorption Coefficient k (in cm^{-1}) of CO_2 in the Region 580 - 1200 Å

λ	k	λ	k	λ	k
582.7	630	692.4	790	708.0	590
85.2	610	92.9	750	08.5	490
90.0	620	93.2	550	09.0	660
605.0	650	93.6	430	09.3	580
10.0	620	94.1	1110	09.8	750
15.0	670	94.4	740	10.6	1770
20.0	600	94.8	900	11.4	800
25.0	590	95.7	480	11.7	650
30.0	590	96.2	540	12.4	490
40.0	580	96.6	1200	12.9	500
50.0	570	97.0	610	13.3	550
59.5	550	97.3	590	13.6	490
65.0	590	97.8	950	14.1	390
70.0	560	98.5	490	14.6	670
75.0	580	99.0	430	14.9	530
77.0	570	99.5	480	15.5	500
80.0	540	700.0	530	16.0	940
82.0	580	00.5	1860	16.3	720
83.0	650	01.4	540	16.8	730
85.0	630	01.9	590	17.5	1390
86.0	590	02.3	1070	18.0	840
87.0	670	03.0	590	19.0	1070
88.7	700	03.6	560	19.4	770
89.3	670	04.1	500	19.9	660
89.6	710	04.6	590	20.4	1000
90.0	530	05.0	560	20.8	810
90.4	780	05.8	480	21.3	540
90.9	540	06.3	530	21.8	1100
91.5	780	07.0	2270	22.3	640
92.1	460	07.6	1000	22.8	480

λ	k	λ	k	λ	k
723.5	650	742.7	620	767.0	1690
24.0	560	43.2	430	67.5	1290
24.5	560	44.8	340	68.8	750
25.0	880	45.1	420	69.3	720
25.5	1120	45.6	780	69.6	680
26.2	2170	46.2	680	70.6	770
27.2	1020	47.0	510	71.3	1090
27.6	1420	47.7	1330	72.5	690
28.0	770	48.5	730	73.6	1450
28.4	630	49.5	460	74.4	950
28.9	530	50.5	350	75.5	770
29.4	940	51.5	480	77.0	660
30.1	600	52.5	8540	77.7	940
30.8	460	53.8	1390	79.0	680
31.6	370	54.2	1740	80.1	1360
32.1	470	54.7	1070	81.1	880
33.1	410	55.5	880	83.0	620
33.6	1050	55.9	850	84.2	550
34.1	570	57.0	620	84.7	630
34.8	1300	57.7	550	86.0	540
35.1	900	58.2	630	87.2	1090
35.5	1060	58.6	930	88.2	730
35.8	600	59.3	850	89.2	680
36.2	560	59.8	800	91.2	520
37.3	400	60.5	1270	93.3	550
38.3	310	60.9	1190	95.1	650
39.1	330	61.8	1120	99.1	500
39.6	570	62.4	1260	801.1	620
40.2	400	62.7	1200	03.0	520
40.7	520	63.0	1240	04.0	520
41.0	520	63.4	1040	05.8	460
41.5	1350	64.8	2210	07.2	520
42.0	660	66.3	1370	08.4	490

λ	k	λ	k	λ	k
809.9	520	892.1	1870	910.3	1700
12.3	460	92.6	1780	11.2	2790
15.7	440	93.6	2180	11.8	2300
16.7	480	94.0	1920	12.1	1930
18.2	390	95.0	2190	12.6	2090
19.2	410	95.7	2030	13.3	1400
20.7	460	96.2	2080	14.1	1980
21.8	410	96.9	2360	14.4	1880
23.2	370	97.4	2110	15.1	2460
24.1	400	97.7	2270	15.6	2790
26.2	350	98.1	2150	16.0	2240
29.9	340	99.0	2470	16.3	2120
30.8	330	900.3	2230	16.7	1130
33.2	360	00.8	2870	17.6	2380
36.0	350	01.1	2500	18.4	1710
42.0	380	01.6	2690	19.3	2780
50.0	440	01.9	2070	19.9	1260
56.0	480	02.4	2320	20.6	2950
60.0	550	02.9	2110	21.2	1140
66.0	680	03.4	2570	22.0	3050
69.5	760	03.7	1910	22.6	1300
74.0	890	04.1	2910	23.2	3500
76.0	980	04.6	2470	23.8	1470
80.0	1150	04.9	2230	24.2	1540
85.6	1450	05.2	2730	24.8	2070
86.3	1580	05.8	2050	25.2	1230
88.0	1650	06.1	2020	26.0	2390
88.9	1660	06.4	2380	26.5	2070
89.4	1720	07.3	2200	27.0	2470
89.9	1650	08.3	1930	27.5	1560
90.7	1730	08.7	2230	28.1	1260
91.2	1940	09.0	1960	28.9	2440
91.6	1700	09.4	2350	29.4	2110

λ	k	λ	k	λ	k
930.0	2400	949.1	1620	975.0	980
30.7	950	49.7	880	76.0	960
31.2	2560	50.7	1840	76.5	1030
32.0	870	51.7	2460	77.2	1220
32.7	1940	52.3	2430	77.7	990
33.3	2640	53.1	2350	78.0	1060
33.6	3000	54.1	1370	78.6	980
34.4	1730	55.1	2530	79.5	1360
34.8	2400	55.9	1110	80.0	1030
35.4	1050	56.4	1870	80.5	780
36.2	1820	56.7	1780	81.2	4180
36.6	1480	57.3	1200	81.5	3950
37.0	1150	58.0	1320	82.5	2440
37.4	2560	58.5	2160	84.0	1010
37.8	2410	59.4	820	85.0	690
38.2	2490	60.5	3080	85.5	680
38.8	1740	61.0	1830	86.0	600
39.2	2650	62.7	1400	86.7	1260
39.9	1590	63.0	2030	87.2	770
40.4	2390	63.4	1420	88.8	1070
41.7	1230	64.0	1540	90.2	700
42.4	2190	64.6	990	90.8	2260
43.7	1560	65.1	890	91.8	2220
44.3	1340	66.0	1010	92.5	1670
44.6	1690	67.0	810	93.5	2390
45.0	1350	68.0	810	94.0	3380
45.4	1480	69.1	1380	95.0	3040
45.8	1210	70.0	1160	96.0	1660
46.1	2330	71.1	910	97.0	990
47.1	1150	71.7	860	98.0	970
47.6	1530	72.5	900	99.0	800
48.3	820	73.2	530	99.5	1250
48.7	1220	73.9	530	1000.2	1060

λ	k	λ	k	λ	k
1001.2	1250	1023.6	840	1045.7	359
01.9	860	24.3	750	46.6	550
03.0	1300	25.3	560	47.1	700
03.6	830	25.7	510	47.8	1520
04.3	670	26.6	690	48.6	1300
05.0	1100	26.9	740	49.5	700
05.5	1220	27.1	700	50.1	357
06.7	1850	27.8	550	50.6	248
07.6	2810	28.2	680	51.9	313
08.1	1630	28.8	550	52.4	338
08.8	1310	29.3	480	54.0	810
10.0	600	30.8	330	54.2	1180
10.5	780	31.3	329	54.7	690
11.0	800	31.9	382	55.2	500
11.7	660	32.3	510	56.3	410
12.3	820	33.1	720	57.0	285
12.5	830	33.6	1040	58.8	410
13.0	710	34.9	1690	60.6	670
13.9	890	35.5	1740	60.9	1510
14.5	1030	36.2	2090	61.1	1880
15.4	770	36.5	1490	61.4	1170
16.4	610	36.9	710	62.0	610
16.9	630	38.0	298	62.6	310
17.8	630	38.2	267	63.6	400
18.3	860	39.5	385	65.1	195
18.8	740	39.9	326	66.6	274
19.4	800	40.5	307	67.6	1090
19.8	1060	40.9	450	67.9	1320
20.4	2360	41.6	540	68.5	1220
20.8	3500	42.5	430	69.7	470
21.1	3530	43.5	276	70.6	530
21.5	2180	44.1	293	71.4	400
22.4	1430	44.9	313	72.2	262

λ	k	λ	k	λ	k
1072.7	330	1111.8	1190	1154.1	12.3
73.2	570	13.4	850	55.8	53
73.8	1070	15.2	850	56.4	139
74.4	480	17.6	1120	57.0	151
75.2	1270	19.0	1610	59.0	24.1
75.9	710	19.7	2120	61.3	7.8
77.7	225	21.3	5140	63.0	5.5
79.2	450	22.4	5980	63.8	7.1
81.0	259	22.7	4850	64.7	29.5
81.8	350	24.7	1170	64.9	34.5
82.9	880	25.0	1240	65.6	29.8
86.0	105	26.1	1520	67.1	7.0
86.8	169	28.2	3030	68.6	5.5
87.5	980	29.0	3330	69.7	3.19
88.6	6800	29.5	2740	70.6	2.46
89.9	820	31.3	1030	71.1	2.21
90.8	373	32.3	610	73.5	5.9
91.1	550	32.8	640	74.6	16.8
91.8	352	33.3	710	75.0	15.9
92.8	560	34.3	540	75.3	10.8
94.7	209	36.6	347	76.6	2.58
97.6	125	37.5	156	77.3	2.12
1100.5	208	38.9	112	78.8	1.40
02.7	388	40.6	550	79.3	1.33
03.2	480	41.8	590	82.0	1.94
03.9	363	43.1	308	83.1	3.17
04.9	228	44.6	116	84.3	2.71
05.4	349	45.3	73	85.6	1.29
05.8	990	47.0	64	87.8	0.89
06.2	227	47.9	85	90.3	1.07
08.3	285	48.6	145	1215.7	2.20
09.9	450	50.9	63		
11.5	1250	53.1	17.8		

Table IV Rydberg Series studied by Price and Simpson[a] and Tanaka et al.[b] ν's are in cm^{-1}; n^* is the effective quantum number by present calculation

n	ν_{obs} (Tanaka et al)	ν_{calc}	$\Delta\nu$	n^*
2	88535	88934	-399	2.20
3	100570	100616	-46	3.21
4	105060	105038	+22	4.23
5	107150	107173	-23	5.21
6	108460	108364	+96	6.33
7	109150	109095	+55	7.32
8	109580	109576	+4	8.23
9	109920	109910	+10	9.26
10	110140	110149	-9	10.17
11	110310	110328	-18	11.11
12	110470	110466	+4	12.26
13	110550	110573	-23	
14	110670	110657	+13	

a. Reference 5

b. Reference 7

Table V. Wave Numbers of Diffuse Bands of CO_2 in the Region 1239 - 1380 A

ν	Δν	ν	Δν
80710		80450	
	650		650
80060		79800	
	680		620
79380		79180	
	640		630
78740		78550	
	620		610
78120		77940	
	670		620
77450		77320	
	650		650
76800		76670	
	640		
76160		---	
	640		
75520		75360	
	650		650
74870		74710	
	680		660
74190		74050	
	640		630
73550		73420	
	590		590
72960		72830	
	530		
72430		---	

a continuum. The present k-values are about 35 %/o lower than those by Sun and Weissler, but in fair agreement with the unpublished result of Cook.[13] In the region 680-780 A, the agreement is good at several wavelengths where comparisons can be made.

The lower curve in Fig. 9 represents the k_i-value of the ionization continuum and does not include the bands. The ionization efficiencies at the band centers are nearly as high as those between the bands, so that, if the bands are included, the k_i-curve will appear very similar in profile to the k-curve. The high ionization efficiencies at the bands indicate that these bands are more or less preionized. This interpretation is consistent with the high-resolution photograph of Tanaka and Ogawa[8] which shows many diffuse bands. The ionization efficiencies in this region range from 60-96 %/o. The lowest yields are found at peaks of sharp bands, while diffuse bands have efficiencies nearly equal to that of the continuum. The present result roughly confirms the work of Wainfan *et al*[12] who, however, obtained results only at a few wavelengths.

b. 780-1000 A Region

Mean absorption coefficients for this region are shown in Figs. 10 and 11, and some values are listed in Table III. In the region 780-840 A, there are several diffuse bands which have been listed by Tanaka *et al*.[7] The wave numbers of the band peaks in the present study agree well with their result except for the first member of their "weak and broad"

series. Our result for this band is 120,150 cm^{-1} compared to their value 120,050 cm^{-1}.

The region 840-890 A appears to be continuous but the region above 890 A contains numerous bands, many of which have been identified as members of five Rydberg series by Tanaka et al.[7] Most of these bands were found in our absorption curve but several were unresolved. Tanaka et al reported that the effective quantum numbers of these series were "rather irregular." However, a recalculation of their result seems to show that the irregularity is not as serious as they have indicated. For example, their "Main Series(1)" is shown in Table IV where ν_{obs} are their observed wave numbers and ν_{calc} are values obtained from the formula:

$$\nu = 111{,}200 - R/(n+0.22)^2$$

The column of $\Delta\nu$ shows that possibly there is a weak perturbation affecting the n=6 and n=7 members of the series. Otherwise, the $\Delta\nu$ appear to be regular, since the lower members usually deviate from the series formula. The above formula gives greater weight to the higher members and the quantum defect is closer to the value 0.21 used by Price and Simpson[5] than the value 0.35 by Tanaka et al. In view of the small $\Delta\nu$ for the higher members, we consider that the error of ±0.03 eV in the ionization potential given by Tanaka et al is rather conservative.

The only published k-values for this region were obtained by Sun and Weissler.[11] Our k-value curve is consistent with some of their k-values but disagree widely at other wavelengths.

For example, in the region around 935 A, their k-value is as low as 94 cm^{-1}, but our result shows a continuum with k-value of 370 cm^{-1}.

The lower curve in Fig. 10 is the extension of the k_1-curve given in Fig. 9. In the region below 890 A, the ionization efficiencies range from 60 to 95 °/o. Since this region is almost without bands, the predominant process should be direct photoionization, with some absorption due to dissociation.

The ionization curve near the threshold (see Fig. 9) shows two close steps at 899.3 and 900.6 A, as in the case of the CS_2 molecule.[12] These apparently correspond to the doublet $^2\Pi_g - ^1\Sigma_g^+$ transition. The above wavelengths correspond to 13.786 and 13.766 eV, respectively, and are almost in exact agreement with the Rydberg series limits obtained by Tanaka et al. In view of this agreement and the resolution of 0.3 A used in the present study, the error in the above values is probably within ±0.003 eV.

c. 1000-1200 A Region

Figs. 12 and 13 summarize the k-values for this region and Table III includes some k-values, especially those at band peaks and minima. This region consists of some very intense bands, the two strongest being the first members of two Rydberg series identified by Price and Simpson.[5] Rathenau[4] observed five sets of progressions with $\Delta\nu$ from 1100 to 1350 cm^{-1} which were confirmed by Tanaka et al;[7] however, the electronic states of these progressions have not been

identified. Our result shows that Rathenau's progressions consist of rather broad diffuse bands. In fact, the k-values at these bands showed almost no pressure dependency, so that the resolution of 0.2 A used for this region was apparently adequate. The diffuseness of these bands may be ascribed to predissociation.

The k-value in this region was previously obtained by Inn et al[10] who used a resolution of about 1 A. The present work confirms most of their results; however, the new curve shows higher peak values, somewhat deeper valleys, and some additional bands in the region below 1120 A. For example, the k-value of the strongest band (at λ=1088.6 A) is now 6800 cm^{-1} compared to the value 3620 cm^{-1} reported by Inn et al. This and other differences can be ascribed to the improvement in resolution. The k-value at Lyman alpha (λ=1215.7 A) was found to be 2.20 cm^{-1} which is about 10 % higher than previous values, 2.0 cm^{-1} by Preston[15] and 1.97 cm^{-1} by Inn et al.

d. 1200-1670 A Region

The absorption curve for this region are summarized in Figs. 13, 14, and 15. The present k-values are in excellent agreement with the k-values tabulated in a report by Watanabe, Zelikoff, and Inn.[16] However, the new results show improvement in the resolution of the diffuse bands, mainly due to the use of greater number of resolved H_2 emission lines.

Price and Simpson[5] have proposed two progressions starting at 1380 and 1368 A with $\Delta\nu$ varying from 1080 to

1350 cm^{-1} corresponding to the ν_1 frequency in the excited state of CO_2. On the other hand, Walsh,[17] in view of the irregularity of this frequency, has suggested the possibility that two different frequencies are involved, one of which may be the bending frequency ν_2 which is roughly half of ν_1 in the ground state. His analysis of the electronic states and a more recent discussion by Mulliken[18] predict an excitation to a bent upper state according to the weak transition $^1B_2 \leftarrow {}^1\Sigma_g^+$ as being the most probable one for the region around 1400 A. However, the question regarding the second weak transition has not been answered; other predicted transitions are either much weaker or are expected at shorter wavelengths.

In view of these theoretical discussions, we have re-examined the diffuse bands for possible arrangements. Although there are no doubts regarding the presence of some bands, other bands have magnitude comparable to the experimental error. There are nearly 80 bands and most of them appear in pairs, with separation of about 130 to 200 cm^{-1}. A rough arrangement consists of a single progression of about 40 double-headed bands for the entire region from 1200 to 1700 A; however, this includes some cases where the existence of a band is questionable. The $\Delta\nu$ between bands is about 600 cm^{-1} in the 1660 A region, decreases to about 530 cm^{-1} in the 1410-1560 A region, and then increases to 640 cm^{-1} in the region 1240-1380 A. The separation of the double peak roughly follows the same trend, decreasing and then increasing. The wave number of some of the bands are listed in Table V.

Although the nature of the double bands is not known, the $\Delta\nu$ between the bands is consistent with the bending frequency ν_2. Thus, it seems possible that the entire region is due to the single predicted transition leading to a bent upper state. The long progression is also consistent with the Franck-Condon principle.

REFERENCES

1. T. Lyman, Astrophys. J. 27, 87 (1908).
2. S. W. Leifson, Astrophys. J. 63, 73 (1926).
3. H. J. Henning, Ann. Physik 13, 599 (1932).
4. G. Rathenau, Z. Physik 87, 32 (1934).
5. W. C. Price and D. M. Simpson, Proc. Roy. Soc. (London) A169, 501 (1938).
6. R. S. Mulliken, J. Chem. Phys. 3, 720 (1935).
7. Y. Tanaka, A. S. Jursa, and F. J. LeBlanc, J. Chem. Phys. 32, 1199 (1960).
8. Y. Tanaka and M. Ogawa, Can. J. Phys. 40, 879 (1962).
9. P. G. Wilkinson and H. L. Johnston, J. Chem. Phys. 18, 190 (1950).
10. E. C. Y. Inn, K. Watanabe, and M. Zelikoff, J. Chem. Phys. 21, 1648 (1953).
11. H. Sun and G. L. Weissler, J. Chem. Phys. 23, 1625 (1955).
12. N. Wainfan, W. C. Walker, and G. L. Weissler, Phys. Rev. 99, 542 (1955).
13. G. R. Cook (private communication, 1965).
14. K. Watanabe, J. Chem. Phys. 22, 1564 (1954).
15. W. M. Preston, Phys. Rev. 57, 887 (1940).
16. K. Watanabe, M. Zelikoff, and E. C. Y. Inn, Geophysical Research Paper, No. 21, Air Force Cambridge Research Laboratory (1953).
17. A. D. Walsh, J. Chem. Soc. (London) 2266 (1953).
18. R. S. Mulliken, Can. J. Chem. 36, 10 (1958).

IV

PHOTOIONIZATION AND ABSORPTION COEFFICIENTS OF NITRIC OXIDE IN THE REGION 580-1100 A

By F. M. Matsunaga, J. S. Sasser, and K. Watanabe

1. INTRODUCTION

The literature on the vacuum UV study of NO is quite extensive and is probably exceeded only by those of H_2, N_2, and O_2. A review article[1] gives about twenty papers published prior to 1957. In the present report, we consider mainly the region 580-1100 A and will not give a complete list of references as most papers deal with the region above 1400 A.

In 1942 Tanaka[2] reported five Rydberg series α, $\beta(0,0)$, $\beta(1,0)$, $\gamma(a)$, and $\gamma(b)$ in the region below 1000 A which converge to three excited states of the NO^+ molecule. Recently, Huber[3] reinvestigated this region and confirmed these series. He found a vibrational Rydberg series $\gamma(1,0)$, five new progressions, and reinterpreted Tanaka's $\beta(1,0)$ series. According to Huber, the convergence limits of the α and γ series correspond to $^3\Sigma^+$ and $^1\Pi$ of NO^+, respectively. The limits of the α, β, and γ series are 114 742, 133 596, and 147 759 cm^{-1} by Tanaka and 114 680, 133 550, and 147 830 cm^{-1} according to Huber.

Although much intensive work has been done for the region above 1400 A, an extensive Rydberg series converging to the ground state of NO^+ has not been unraveled. Huber and Miescher[4] have summarized the known Rydberg states of NO for

this region. The first ionization potential was found to be 9.25 ±0.02 eV by photoionization measurements.[5] It was also reported[5] that the ionization potential may be determined by subtracting the energy of the 0-0 transition (73,084 cm^{-1}) of Miescher-Baer bands[6,7] from the energy of the γ series limit (147,759 cm^{-1}) of Tanaka. This value is 9.258 eV, or, if Huber's limit is used, 9.267 eV. The small discrepancy of about 0.017 eV between the photoionization value and Huber's value may be due to the possibility that the photoionization measures the transition $^2\Pi_{3/2} - {}^1\Sigma^+$.

The absorption coefficients of NO in the region below 1100 A have been reported by Sun and Weissler[8] down to 374 A and by Granier and Astoin[9] down to 150 A. However, both groups used line sources and photographic photometry. Recently, Metzger and Cook[10] obtained both absorption and photoionization data using the helium continuum and photoelectric techniques. Photoionization cross sections at few wavelengths were reported by Walker and Weissler.[11]

The present study is an extension of our previous work[12] for the region 1060-1350 A using 0.2 A resolution. Both absorption coefficient and photoionization efficiency were obtained in the region 580-900 A with 0.3 A resolution and in the region 860-1100 A with 0.4 A resolution.

2. EXPERIMENTAL

The apparatus and experimental procedure used for the absorption measurement of NO were the same as those described in Part II.

Nitric oxide gas from a cylinder was purified by eleven successive fractional distillation in vacuum and kept in liter flasks. Gas pressures from 0.009 to 0.24 mm Hg were used in a windowless cell of 13.6 cm length for the spectral region 860-1100 A, where the H_2 light source was used. Gas pressures from 0.012 to 0.23 mm Hg were used in a 11.5 cm cell for the region 580-910 A, where the Hopfield continuum was used. For ion current measurements the cell lengths were 27.1 and 54 cm, and gas pressures were from 0.05 to 0.46 mm Hg. The voltages across the parallel plates of the ion chamber were from 15 to 20 V. Xenon gas served as the reference ionization gas for measurements of absolute intensity in the region below 910 A, but a platinum photocell calibrated against a thermocouple was used for the region 860-1100 A. In the overlapping wavelength region, the two methods gave consistent results.

The estimated experimental errors in the k-value were 5 to 15 °/o and in the k_1-value, 15 to 25 °/o. The errors were relatively large in the region below 700 A, where the source intensity was low.

3. RESULTS AND DISCUSSION

The mean absorption coefficients of NO for the region 580-1100 A are listed in Table VI and summarized in Figs. 16 through 19. The absorption spectrum is in good agreement with the photographs by Tanaka[2] (1-m grazing incidence spectrograph) and Huber[3] (1-m and 3-m instruments). Nearly all bands reported by them can be seen in our curve, but

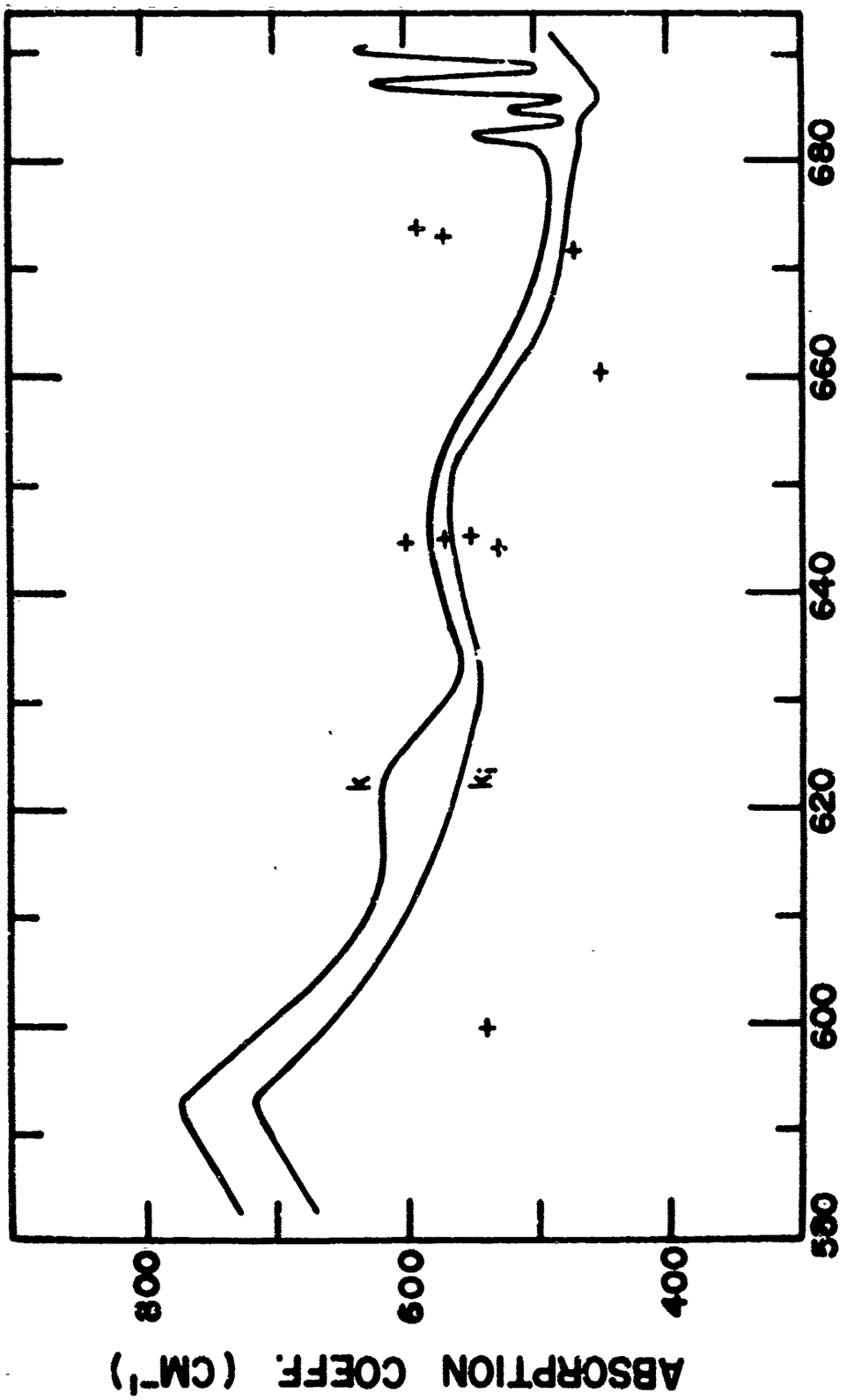

Figure 16. Absorption and photoionization coefficients of NO in the region 580 - 680 A. + are k-values by Sun and Weissler

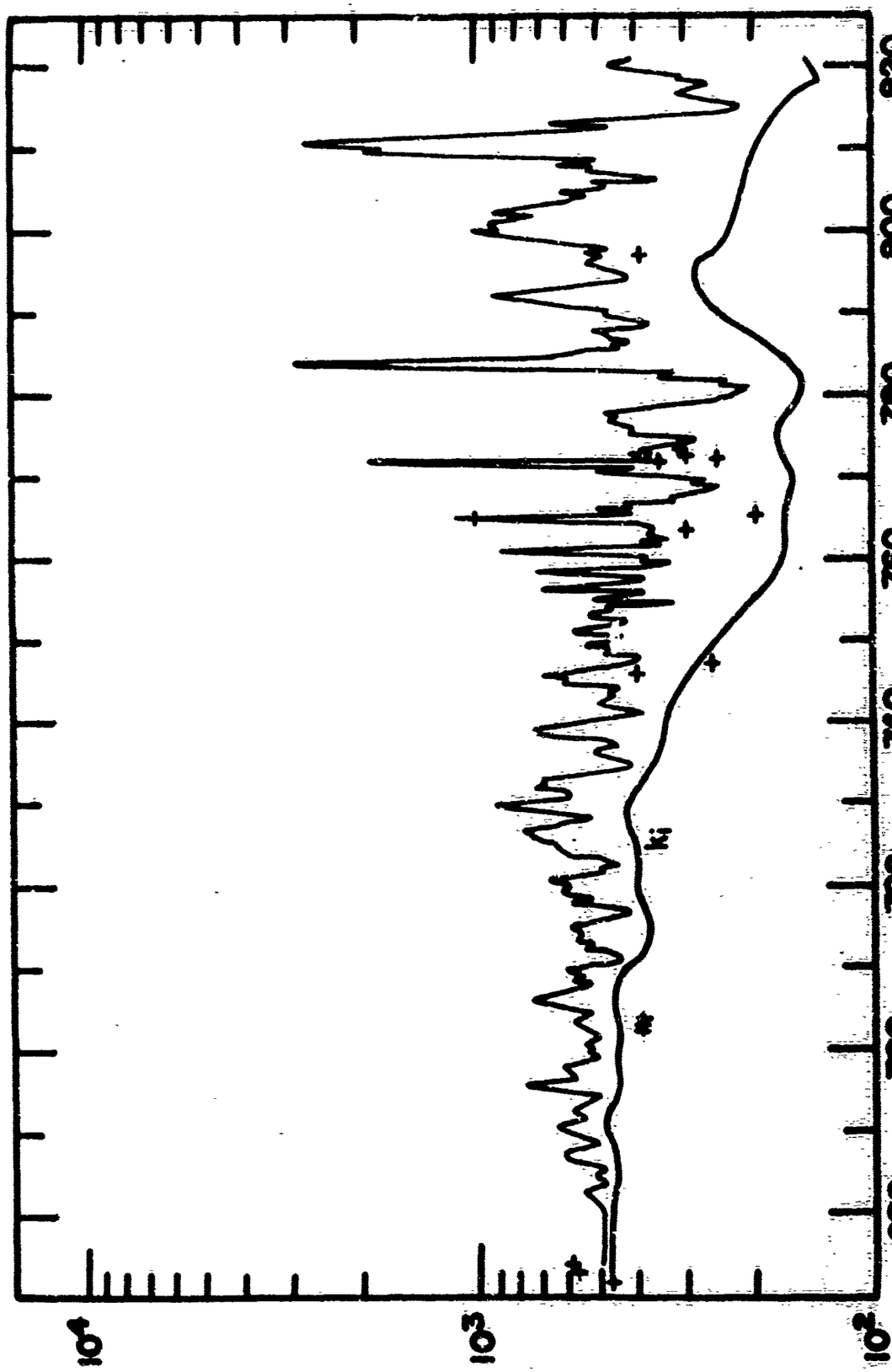

Figure 17. Absorption and photoionization coefficients of NO in the region 680 - 820 A

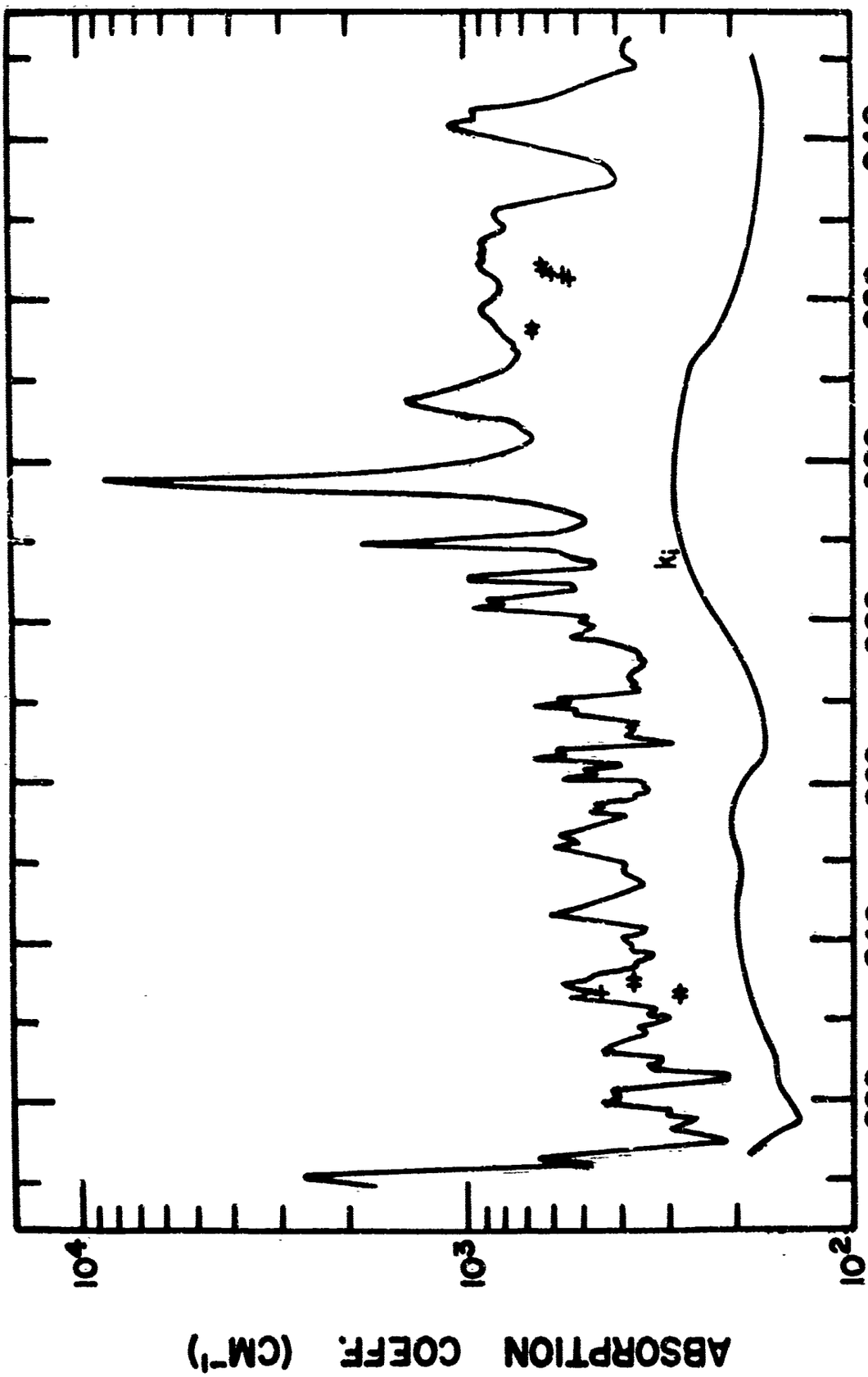

Figure 18. Absorption and photoionization coefficients of NO in the region 820 - 950 A

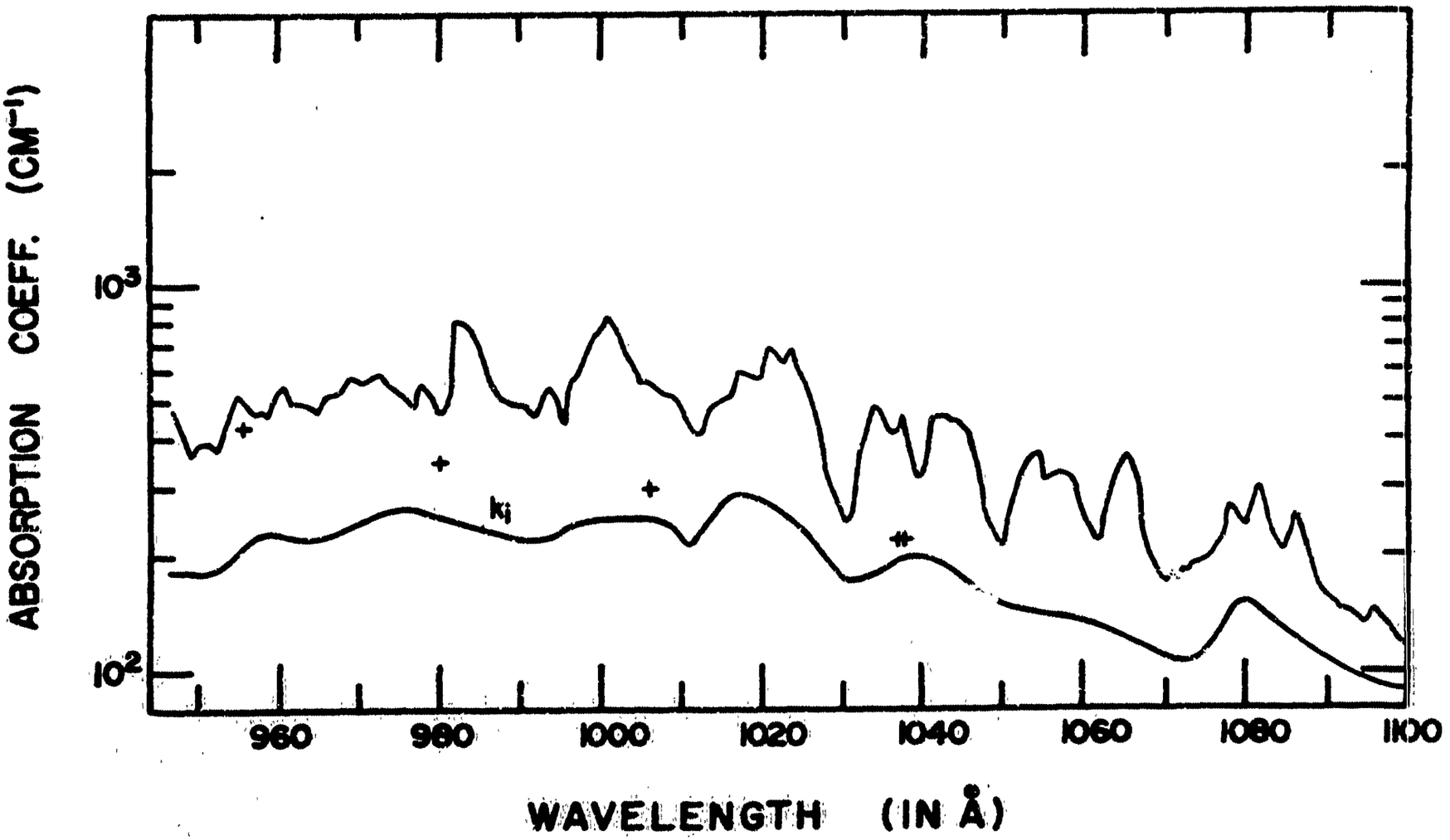

Figure 19. Absorption and photoionization coefficients of NO in the region 950 - 1100 A

Table VI. Absorption Coefficient k (in cm^{-1}) of NO in the Region 580 - 1100 Å

λ	k	λ	k	λ	k
582.5	730	701.3	500	724.4	630
92.5	770	02.1	510	25.3	650
602.5	680	03.5	580	25.6	720
12.5	620	04.6	520	26.0	730
22.5	620	06.0	740	26.5	770
32.5	560	07.9	530	27.4	600
42.5	580	08.2	580	27.7	600
52.5	580	08.5	550	28.1	520
61.9	520	09.1	610	29.2	910
72.0	490	10.6	440	29.5	820
81.1	500	11.9	550	29.9	780
82.4	550	12.4	520	30.7	590
83.7	480	13.0	570	31.3	600
84.7	520	13.8	550	31.7	740
85.7	480	14.4	590	32.1	690
86.8	610	16.7	420	32.4	690
87.4	630	17.5	560	34.1	430
88.6	500	18.1	600	34.5	410
90.4	640	18.5	520	34.8	420
91.7	540	18.9	610	35.3	490
92.7	590	19.3	620	35.9	510
94.3	490	19.8	590	36.4	450
95.7	770	20.3	670	36.8	440
96.8	570	21.8	480	37.4	480
97.9	620	22.0	490	37.9	680
99.1	500	22.5	440	38.6	730
99.5	510	23.1	480	40.3	390
99.9	540	23.4	500	41.0	380
700.2	520	23.7	590	41.3	440
00.6	540	24.0	620	41.9	500

λ	k	λ	k	λ	k
742.9	450	758.4	390	773.6	331
43.2	470	58.7	370	74.0	278
43.7	440	59.2	320	74.6	277
44.4	610	59.5	380	75.2	410
44.7	590	59.9	370	75.7	396
45.2	690	60.5	880	76.0	420
45.8	550	61.2	340	76.6	460
46.1	530	61.5	390	76.9	430
47.0	400	61.8	320	77.3	480
47.5	390	62.4	370	79.6	226
47.8	385	62.7	370	80.2	222
48.1	480	63.3	350	80.7	201
48.6	450	63.9	380	81.2	241
49.0	540	64.6	1140	81.5	233
49.4	460	65.2	400	81.9	342
49.7	440	65.5	500	82.4	314
50.0	420	66.0	400	83.6	2910
50.5	580	66.3	420	84.3	610
50.8	550	66.6	310	85.1	560
51.1	560	66.9	320	85.8	460
51.9	410	67.3	284	86.2	410
52.3	520	67.6	282	86.7	450
52.8	510	68.4	239	87.1	450
53.2	450	68.7	284	87.4	510
53.5	480	69.2	260	88.0	387
54.1	316	70.2	500	88.6	361
54.6	510	70.6	394	89.4	470
55.3	380	71.3	1890	90.1	460
55.9	700	72.1	356	92.1	910
56.9	380	72.4	420	93.9	410
57.1	380	72.7	355	94.4	430
57.4	370	73.0	390	95.5	530
57.9	710	73.3	340	96.5	480

λ	k	λ	k	λ	k
796.9	530	815.0	213	828.7	353
97.4	460	15.5	254	29.1	349
97.7	480	15.8	251	29.4	377
98.0	480	16.2	308	30.5	293
98.4	550	16.5	305	31.1	355
99.3	580	16.8	303	31.6	328
99.7	1020	17.3	296	32.5	352
800.0	880	17.6	256	32.8	430
00.3	930	17.9	266	33.2	560
01.4	710	18.2	309	33.7	490
02.1	910	18.5	298	34.0	460
02.7	730	18.8	319	34.3	560
03.7	580	19.5	460	34.6	550
04.1	520	19.9	410	35.2	600
04.4	610	20.2	410	35.6	490
04.8	530	20.5	400	35.9	470
05.1	470	20.9	430	37.3	364
05.4	510	21.2	383	37.6	369
06.0	344	21.6	399	38.5	325
06.5	410	22.5	214	39.3	374
07.0	520	23.0	212	39.7	367
07.3	510	23.7	328	40.0	382
07.8	630	24.0	321	40.5	390
08.3	500	24.5	351	41.5	342
09.0	950	24.9	316	42.0	393
09.4	1920	25.3	335	42.5	510
09.7	1730	25.6	348	42.9	630
10.6	2730	26.2	470	43.5	620
12.2	470	26.6	450	44.6	470
12.7	650	26.9	430	47.0	350
13.2	410	27.2	430	48.5	400
13.5	410	27.8	405	48.8	397
14.5	216	28.1	400	49.7	395

λ	k	λ	k	λ	k
851.3	610	868.6	530	883.4	560
52.0	520	68.9	520	84.0	520
52.8	590	69.4	690	84.3	530
54.3	500	70.0	520	85.0	1020
55.6	387	70.3	600	85.3	960
56.3	500	71.1	399	85.7	900
56.7	430	71.4	357	86.3	550
57.0	470	71.7	372	86.8	460
57.6	420	72.1	366	87.3	500
57.9	361	72.8	375	87.6	510
58.2	366	73.1	387	87.9	520
59.1	335	74.0	365	88.4	620
59.5	351	74.3	342	89.4	1900
59.8	350	74.8	339	90.9	680
60.2	353	75.1	356	92.0	490
60.6	580	75.5	356	92.7	480
61.1	460	75.8	379	94.1	660
61.5	520	76.1	381	94.5	660
62.0	430	76.2	379	95.6	1020
62.3	396	76.5	410	96.6	2650
62.9	680	76.8	410	96.9	4480
63.3	560	77.9	520	97.3	8990
63.7	590	78.2	550	98.0	4220
64.0	420	78.6	530	98.7	2130
64.4	354	78.9	510	99.6	1120
64.7	308	79.4	460	901.0	750
65.0	289	79.8	520	01.5	710
65.3	304	80.2	480	02.4	670
65.9	389	81.1	625	02.8	660
66.3	362	81.8	980	03.7	680
66.7	386	82.3	810	05.1	760
67.1	352	82.5	920	06.1	1100
67.7	372	83.0	750	06.8	1340

λ	k	λ	k	λ	k
907.6	1450	940.2	830	976.2	490
08.5	1210	41.6	1110	76.7	480
10.5	860	42.2	920	77.5	560
11.4	790	43.2	970	78.5	530
12.1	770	44.8	600	79.2	500
13.4	730	45.2	580	80.1	460
14.2	760	46.0	540	81.3	540
14.8	750	46.7	490	82.1	810
16.0	810	48.1	410	83.8	790
17.0	840	49.1	359	84.6	720
17.8	840	49.7	390	86.1	560
19.0	930	50.9	394	86.9	520
20.0	880	52.3	373	88.5	500
21.4	790	53.7	451	89.6	490
22.3	820	54.8	520	90.6	490
23.4	890	55.7	490	91.7	450
24.0	890	56.9	460	93.3	540
24.4	940	57.8	460	94.2	520
24.8	920	58.4	450	95.2	440
25.1	880	60.0	540	96.1	460
25.8	900	60.7	550	96.6	460
26.0	890	61.7	490	97.6	620
26.8	930	62.8	500	98.8	720
28.8	780	64.1	490	1000.0	760
30.0	840	64.8	470	00.7	830
30.3	870	66.0	520	01.9	760
31.5	820	67.5	530	02.6	690
33.0	570	68.3	570	04.0	600
34.6	410	69.2	580	04.6	560
35.6	410	70.3	560	05.5	570
36.2	420	72.5	590	06.2	550
36.9	430	73.4	560	07.6	530
37.6	490	74.6	540	08.8	520

λ	k	λ	k	λ	k
1009.4	500	1039.9	327	1069.9	164
10.0	460	40.9	450	70.7	173
10.8	430	42.5	460	71.4	166
11.5	410	42.9	450	72.2	176
12.3	420	43.5	440	72.7	177
13.5	490	44.1	440	73.2	184
14.2	500	45.3	410	73.9	183
16.0	520	46.6	327	75.3	193
16.9	600	47.1	290	76.0	198
17.8	590	47.8	247	77.0	202
19.4	574	49.5	209	77.8	257
20.8	690	50.1	227	79.8	226
22.4	620	50.6	255	81.6	288
23.4	680	52.4	345	83.0	217
24.7	590	54.2	370	84.6	198
25.7	520	54.7	311	86.1	243
27.1	395	55.5	318	86.8	230
28.2	319	56.4	327	87.7	195
29.3	269	58.8	305	88.7	170
30.2	240	59.5	236	90.0	153
30.8	246	61.7	199	91.1	146
31.9	370	62.6	248	91.7	140
33.6	480	63.6	291	92.7	140
34.3	460	65.1	351	93.4	138
35.5	400	66.4	285	94.6	132
36.5	410	67.0	231	95.9	140
37.2	450	67.6	204	97.1	132
38.1	379	68.5	180	97.9	130
39.1	201	68.9	174	99.5	119

Table VII. Comparison of k-values (in cm^{-1}) for the α, β, and γ Rydberg series of Nitric Oxide. Tanaka's wavelengths are used, except for four by Huber.

	α - Series			β - Series			γ - Series		
n	λ(A)	Cook Metzger	Present	λ(A)	Cook Metzger	Present	λ(A)	Cook Metzger	Present
2	982.5 H		810	897.3 H		8990	800.5	785	930
3	931.1 H	1000	870	810.8	2000	2730	729.0	648	910
4	907.5	1210	1450	783.5	1900	2910	705.9	620	740
5	896.0	6200	8990	771.1	1160	1890	695.8	585	770
6	889.3	1600	1900	764.5	910	1140	690.0	580	640
7	885.0	860	1020	760.2	630	880	686.5	570	620
8	882.1	775	920	757.6	550	710	684.3		520
9	880.1	630	980	755.8	510	700	682.7		550
10	878.6		550	754.6		510			
11				753.6 H		480			

there are also numerous unidentified bands.

Only a few of the present k-values can be compared with the results by Sun and Weissler[8] and by Granier and Astoin[9] because these workers used line sources. The k-value obtained by Sun and Weissler are indicated by crosses in Figs. 16-19. The results are in fair agreement at some wavelengths but discrepancies of factor of two or more are noted at other wavelengths. Our results suggest that the band-like structures shown in the curve of Granier and Astoin are due mainly to scatter of experimental values rather than to band structure.

The present results are most consistent with the absorption curve obtained by Metzger and Cook.[10] The k-values are in good agreement in the continuous region 600-680 A, at weak bands, and regions between bands. However, discrepancies are noted at the peaks of strong bands, as shown in Table VII for the α, β, and γ Rydberg bands. These discrepancies may be ascribed to the difference in the optical resolution used by the two groups of workers. The present result also shows more detail in the absorption curve.

The strongest band in the region 580-1100 A is the 896 A band which has a k-value of 8990 cm^{-1}. Tanaka identified this band as a member (n=5) of the α series. On the other hand, Huber reported this band as two bands with wavelengths 897.3 A and 897.7 A and identified them as $\beta(2)$ and $\alpha(5)$, respectively. Our low pressure data did not resolve this structure; however, the intensity of this band is sufficiently high for two overlapping bands. Taking into account the anomaly of the 897 A band, we infer from Table VII that the strongest band in the

α series is n=5 and β series n=3 or 4. Thus the result suggests that a considerable change in the internuclear distance occurs during the transition from the ground state of NO to the upper states of the α and β series. On the other hand, the γ series probably involves a nearly vertical transition.

The k_1-curve shown in Figs. 16-19 was obtained by drawing a smooth curve through points corresponding to the minima in the k-curve. If the k_1-values for band peaks are included, the lower curve will appear very similar to the k-curve as shown by Metzger and Cook. Hence, the bands are more or less preionized throughout the region from 680 to 1100 A. The ionization efficiencies range from 87 to 98 % in the region 580-690 A, including the few bands shown in Fig. 16. The ionization efficiency decreases toward the long wavelength side and the range is from 66 to 93 % in the 690-740 A region. This range includes band peaks. Above 750 A, the efficiencies were mostly in the range 30-60 %, but some bands showed efficiencies of about 25 %. Values of 50 to 70 % found at minima of the absorption curve indicate the presence of dissociation continua in the region 750-1050 A. Many bands in this region are rather diffuse and we may ascribe the diffuseness to both predissociation and preionization.

According to Metzger and Cook[10] the photoionization efficiency is about 78 % at 600 A, decreases steadily to about 40 % at 760 A, and is about 35 % up to 950 A.

Walker and Weissler[11] report about 70 % at 700 A and about 50 % in the region 800-1200 A. The present result shows somewhat larger variations, but on the average, is in good agreement with the result of the latter work.

REFERENCES

1. K. Watanabe, Advances in Geophysics, Vol. 5 (Academic Press, New York, 1958) p.190.
2. Y. Tanaka, Sci. Papers Inst. Phys. Chem. Res. (Tokyo) 39, 456 (1942).
3. K. P. Huber, Helv. Phys. Acta 34, 929 (1961).
4. K. P. Huber and E. Miescher, Helv. Phys. Acta 36, 257 (1963).
5. K. Watanabe, J. Chem. Phys. 22, 1564 (1954).
6. E. Miescher and P. Baer, Nature 169, 581 (1952).
7. Y. Tanaka, J. Chem. Phys. 21, 562 (1953).
8. H. Sun and G. L. Weissler, J. Chem. Phys. 23, 1372 (1955).
9. J. Granier and N. Astoin, Compt. rend. 242, 1431 (1956).
10. P. H. Metzger and G. R. Cook, Report No. ATN-63(9218)-7, Aerospace Corporation, Los Angeles, 1963.
11. W. C. Walker and G. L. Weissler, J. Chem. Phys. 23, 1962 (1955).
12. K. Watanabe, H. Sakai, J. Mottl, and T. Nakayama, Scientific Report No. 4, AFCRC-TN-58-657, 1958.

V

MISCELLANEOUS TOPICS

By F. M. Matsunaga and K. Watanabe

1. ABSORPTION COEFFICIENTS OF H_2 IN THE REGION 600-840 A

The electronic states of H_2 have been studied both theoretically and experimentally by numerous investigators. References to early work are given in treatises by Herzberg[1] and Richardson[2] and a paper by Tanaka.[3] More recent results and references are found in papers by Monfils[4] and Namioka.[5]

Absorption coefficients of H_2 in the region below 1000 A have been reported by Lee and Weissler[6] at about 50 wavelengths and by Bunch et al[7] at a few wavelengths. Recently, Cook and Metzger[8] reported a much more detailed spectrum obtained with the Hopfield continuum source. Photoionization efficiencies were obtained at nine wavelengths by Wainfan et al[9] and continuously from 580 to 800 A by Cook and Metzger.[8]

The present work is similar to the work of Cook and Metzger except that we have used somewhat better resolution, about 0.3 A in place of 0.5 A. The apparatus and experimental methods are described in part II. H_2 pressures from 0.035 to 1.4 mm Hg were used in cells of 11.5 and 54 cm length. The ionization efficiencies were also determined with xenon as a reference gas.

The absorption coefficients for the region 600-840 A are summarized in Figs. 20 and 21. The k-values in the region above 780 A showed a strong pressure dependence. Since this region consists of many sharp bands, we can ascribe the

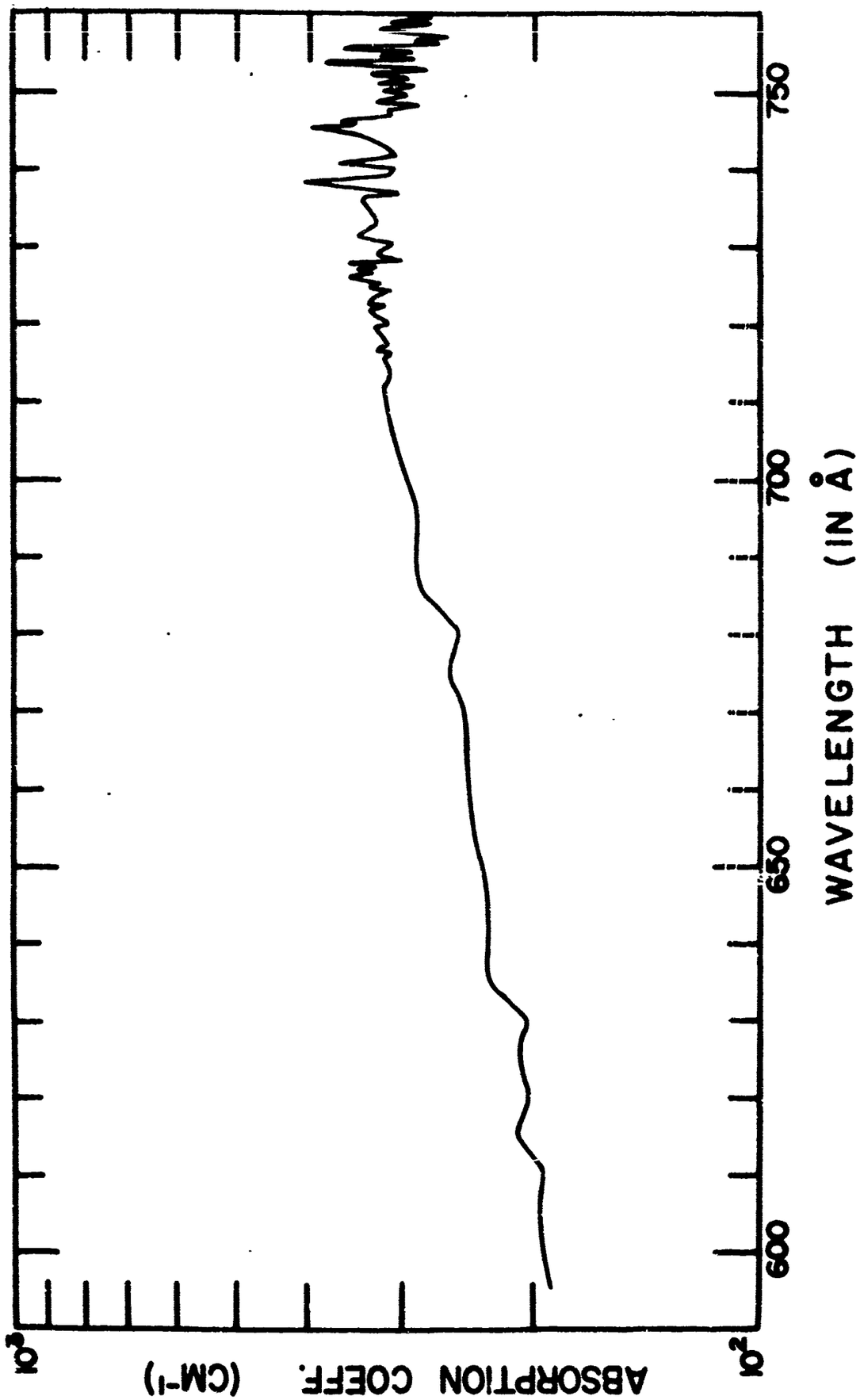

Figure 20. Absorption coefficient of H_2 in the region 590 - 760 A

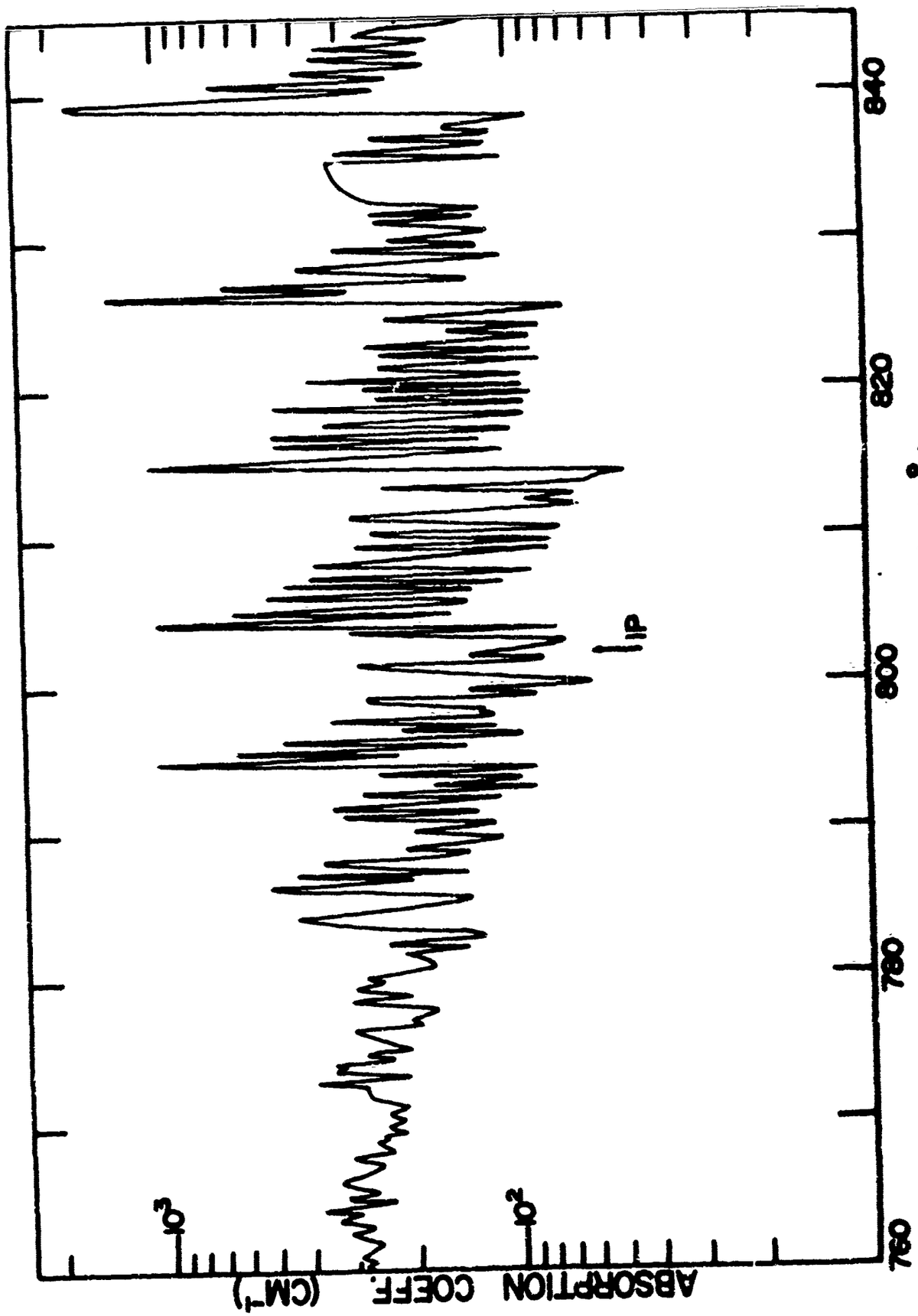

Figure 21. Absorption coefficient of H_2 in the region 760 - 840 A

apparent pressure effect to insufficient resolution. Low pressure data were used for the peaks of the bands and high pressure data for the valleys. Even so, the maximum k-values are probably too low and the k-value for this region should be regarded as semi-quantitative. In the region below 780 A, the k-values at the various bands showed no pressure dependence, with the exception of the peaks at 772.9 and 774.1 A.

The k-values for the region 600-780 A agree very closely with the curve by Cook and Metzger;[8] however, the present curve shows many additional bands in the region 720-780 A. Similarly in the region above 780 A, the present curve shows a much more complex band structure. Furthermore, the peak k-values are about a factor of two larger and the deepest minima are about a factor of two or three smaller. These differences may be ascribed to improved resolution. Our result shows that further improvement in resolution is required to obtain quantitative k-values in the region above 780 A.

The ionization efficiency of 100 $^{o}/o$ obtained for the region 590-73(A confirms the result of Cook and Metzger. In the region 730-780 A, the efficiency is about 100 $^{o}/o$ at minima of the absorption curve, but the efficiency is as low as 60 $^{o}/o$ at band peaks. In the region 780-804 A, the lowest efficiency of about 19 $^{o}/o$ is identified with the $v'=7$ band (794.6 A) of the D→X transition, but at the ionization threshold at 803.7 A the efficiency is about 75 $^{o}/o$. Thus the present data show that many of the bands in the region below 803.7 A are not preionized.

2. IONIZATION POTENTIAL OF COS

Price and Simpson[10] and Tanaka et al[11] have studied the absorption spectrum of COS to identify one or more Rydberg series converging to the first ionization limit; however, no conclusive identification was obtained. Tanaka et al suggested two limits, about 10.5 eV and 11.23 eV. Preliminary photoionization measurements by Matsunaga[12] gave a value of about 11.17 eV, but there was some doubt regarding the purity of the gas sample.

In the present study, COS from Matheson Company was purified by vacuum distillation, and both k value and ionization efficiencies were measured. The H_2 source was used with a resolution of 0.5 A. Gas pressures of 0.35-2.0 and 0.04-0.7 mm Hg in a 10.5 cm cell were used in the ionization and absorption measurements, respectively. Nitric oxide served as the reference gas for photoionization efficiency.

The k and k_1 curves for COS in the region 1065-1125 A are shown in Fig. 22. The arrows indicate the proposed doublet limit at 11.16 and 11.18 eV. The k_1 curve shows a very sharp drop at about 1111 A, indicating a nearly vertical ionization potential. On the longer wavelength tail there is a minor ledge at $\Delta\nu$~500 cm^{-1} from the arrow at 1111 A. This value is very close to the $\Delta\nu$ of 527 cm^{-1} reported by Penny and Sutherland.[13] Thus the photoionization measurement provides strong evidence that the ionization potential of COS is 11.16 eV and confirms the preliminary value.

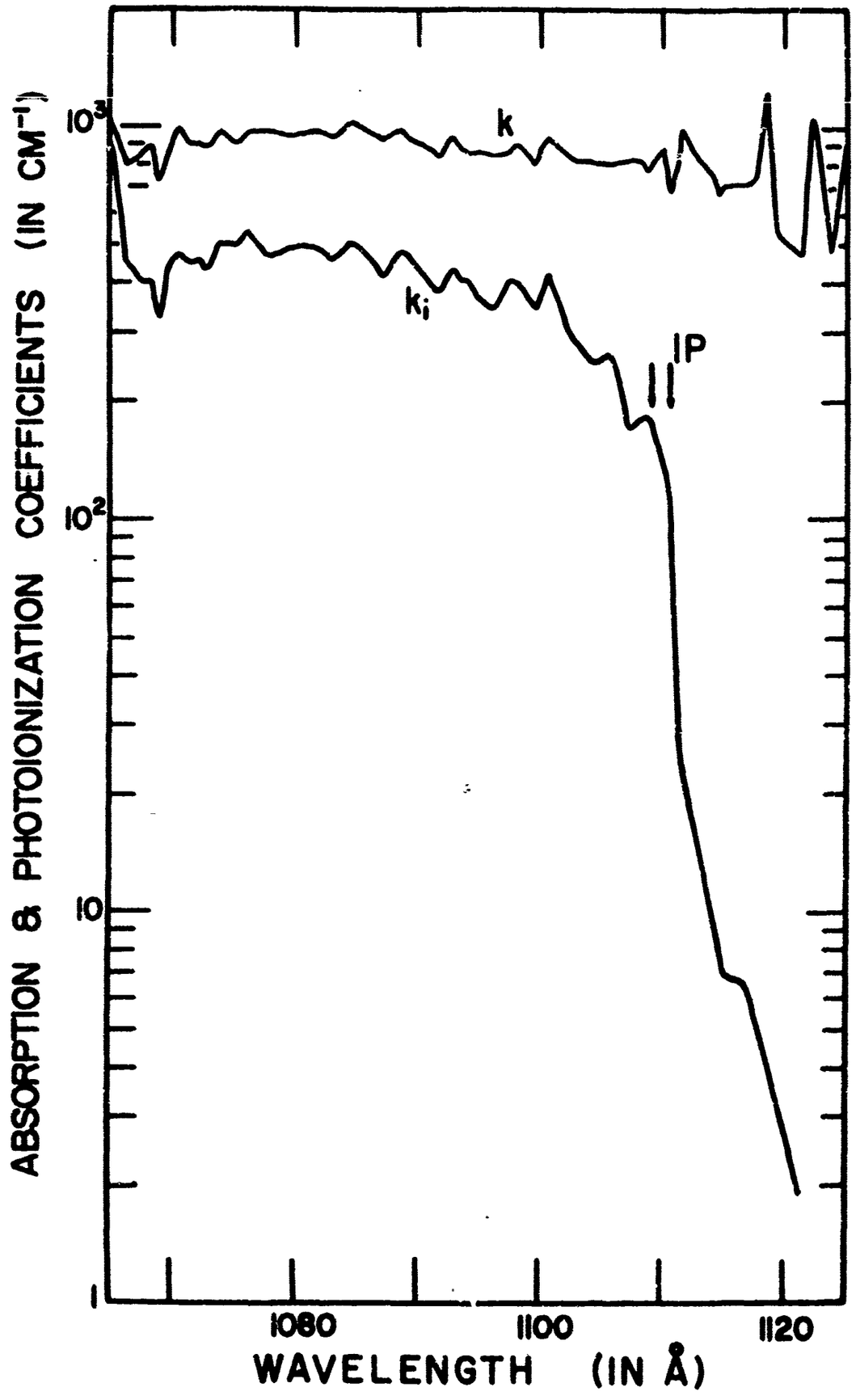

Figure 22. Absorption and photoionization coefficients of COS in the region 1065 - 1125 A

3. FLUORESCENCE AND SCATTERING OF SOME GASES UNDER EXCITATION OF 1100-2200 A RADIATION

An exploratory study was made to detect fluorescence and scattering from O_2, CO_2, NO, and NH_3 under excitation by dispersed radiation in the region 1100-2200 A. The gas sample at various pressures was contained in a chamber with LiF window located at the exit slit of the monochromator. The band width of the dispersed H_2 spectrum was about 20 A. A Dumont 6291 photomultiplier was attached to the chamber, and it viewed the chamber in a direction normal to the beam from the exit slit. In some measurements the glass plate in front of the photomultiplier was coated with sodium salicylate to detect radiation shorter than 3000 A.

Only qualitative results were obtained and are summarized briefly in the table below:

	Detected Radiation	
Gas	$\lambda > 3000$ A	$\lambda < 3000$ A
O_2	none	at 1117, 1190, 1216 A
NO	at 1577 A	at about 20 wavelengths including gamma bands
CO_2	none	at 1216, 1240, 1254, 1277 A
NH_3	1100-1160 A	1100-1440 A

Gill and Heddle[14] and Marmo and Mikawa[15] have reported relative scattering cross sections of some gases for the Lyman alpha radiation; however, available data are extremely meager. The present exploratory study suggests that further study of fluorescence and scattering is desirable in the vacuum ultraviolet region.

REFERENCES

1. G. Herzberg, Spectra of Diatomic Molecules (D. Van Nostrand Company, Inc., New York, 1950).
2. O. W. Richardson, Molecular Hydrogen and Its Spectrum (Yale University Press, New Haven, Connecticut, 1934).
3. Y. Tanaka, Sci. Papers Inst. Phys. Chem. Res. (Tokyo) 42, 49 (1944).
4. A. Monfils, Bull. Acad. Roy. Belg. (Sciences) 47, 585, 599 and 816 (1961).
5. T. Namioka, J. Chem. Phys. 40, 3154 (1964); 41, 2141 (1956).
6. P. Lee and G. L. Weissler, Astrophys. J. 115, 570 (1952).
7. S. M. Bunch, G. R. Cook, M. Ogawa, and A. W. Ehler, J. Chem. Phys. 28, 740 (1958).
8. G. R. Cook and P. H. Metzger, J. Opt. Soc. Am. 54, 968 (1964).
9. N. Wainfan, W. C. Walker, and G. L. Weissler, Phys. Rev. 99, 542 (1955).
10. W. C. Price and D. M. Simpson, Proc. Roy. Soc. (London) A165, 272 (1938).
11. Y. Tanaka, A. S. Jursa, and F. J. LeBlanc, J. Chem. Phys. 32, 1205 (1960).
12. F. M. Matsunaga, unpublished material.
13. W. G. Penny and G. B. B. M. Sutherland, Proc. Roy. Soc. (London) A156, 654 (1936).
14. P. Gill and D. W. O. Heddle, J. Opt. Soc. Am. 53, 847 (1963).
15. F. F. Marmo and Y. Mikawa, Bull. Am. Phys. Soc. 9, 626 (1964).